Tectonic implications of the lithospheric structure across the Barents and Kara shelves

Jan Inge Faleide[1*], Victoria Pease[2], Mike Curtis[3], Peter Klitzke[4], Alexander Minakov[1], Magdalena Scheck-Wenderoth[5], Sergei Kostyuchenko[6], Andrei Zayonchek[7]

[1]*Centre for Earth Evolution and Dynamics (CEED), Department of Geosciences, University of Oslo, Oslo, Norway;* [2]*Department of Geological Sciences, Stockholm University, Stockholm, Sweden;* [3]*CASP, Cambridge, UK;* [4]*Federal Institute for Geosciences and Natural Resources (BGR), Hannover, Germany;* [5]*Helmholtz Centre Potsdam, GFZ German Research Centre for Geosciences, Potsdam, Germany;* [6]*VNIIGeofizika, Moscow, Russia;* [7]*Rosgeo, Moscow, Russia*

Abstract

We present, summarize and discuss the lithosphere structure and evolution of the wider Barents-Kara Sea region, based on compilation and integration of geophysical and geological data. Regional transects are constructed at both crustal and lithospheric scales based on the available data and a regional 3D model. The transects, which extend onshore and into the deep oceanic basins are used to link deep and shallow structures and processes, as well as to link offshore and onshore areas.
The study area has been affected by numerous orogenic events: (1) Precambrian-Cambrian (Timanian), (2) Silurian-Devonian (Caledonian), (3) Latest Devonian-earliest Carboniferous (Ellesmerian/Svalbardian), (4) Carboniferous-Permian (Uralian), (5) Late Triassic (Taimyr, Pai Khoi, Novaya Zemlya), (6) Paleogene (Spitsbergen/Eurekan). It has also been affected by at least three episodes of regional-scale magmatism, so-called large igneous provinces (LIPs): (1) Siberian Traps (Permian-Triassic transition); (2) High Arctic Large Igneous Province (HALIP; Early Cretaceous); (3) North Atlantic (Paleocene-Eocene transition). Additional magmatic events occurred in parts of the study area in Devonian and Late Cretaceous times.
Within this geological framework, basin development is integrated with regional tectonic events and stages in basin evolution are summarized. We further discuss the timing, causes and implications of basin evolution. Fault activity is related to regional stress regimes and reactivation of pre-existing basement structures. Regional uplift/subsidence events are discussed in a source-to-sink context and related to their regional tectonic and paleogeographic settings.

Keywords:

Arctic; lithosphere; crustal structure; basin architecture and development;

The tectonic evolution of the Arctic is one of the most controversial on Earth due to its geological complexity, as well as the logistical challenges associated with working in the far north. The Barents and Kara shelf regions comprise one of the broad shelf/margin provinces bounding the Arctic Ocean (Fig. 1). It is probably the best known of these shelf regions because of its more favourable ice conditions and long-term exploration activity. Most of the Barents Sea is covered by a dense grid of seismic reflection data and a number of deep seismic refraction profiles. More than 100 exploration wells have been drilled in the Norwegian part of the Barents Sea. About 60 wells have been drilled on the Russian side. Geological information for the region also comes from the onshore geology of the archipelagos of Svalbard, Franz Josef Land, Novaya Zemlya, and Severnaya Zemlya, as well as the mainland of Arctic Norway and Russia. Field work on Svalbard has been an important and integral aspect for understanding the Norwegian part of the Barents Sea (e.g., Dallmann, 2015; Piepjohn et al., 2016; Piepjohn & von Gossen, *this volume*). On the Russian side, several joint German-Russian and Swedish-Russian expeditions (land and sea) have occurred in recent years (e.g., Pease, 2013; Pease, 2012), contributing to a better understanding of the region.

Much new data have been acquired in relation to the United Nations Convention on the Law of the Sea which allows sovereign Arctic coastal states to expand the nautical limits of their economic territory. The new geological and geophysical data have provided insights into the structure and evolution of the Arctic Ocean and surrounding continental margins and shelves. Data have been shared across national/political borders leading to closer collaboration between research partners. Despite the new data there are still major challenges to understanding the geological evolution of the region prior to the formation of the oceanic basins of the Arctic Ocean. At present, no single model fully and consistently explains the tectonic development of the Arctic. While the kinematics associated with its Cenozoic evolution is rather well understood, many questions remain regarding the Cretaceous and earlier evolution. The main element in reconstructing the tectonic evolution of any region is the lithosphere: continental and oceanic. Therefore, understanding the lithosphere, its composition, thermal evolution and paleostress history, is critical for geological reconstructions.

Several generations of regional 3D crustal and lithospheric models have been constructed for the Barents-Kara Sea region (Fig. 2) based on compilation and integration of the geological/geophysical database (Ritzmann et al., 2007; Levshin et al., 2007; Hauser et al., 2011; Klitzke et al., 2015). The most recent 3D model of Klitzke et al. (2015) has been used to constrain the thermal evolution and long-term rheological behaviour of the lithosphere (e.g., Gac et al., 2016; Klitzke et al., 2016).

We discuss the lithospheric structure and evolution of the Barents-Kara Sea region, based on compilation and integration of relevant geophysical and geological data. Regional transects are constructed at both crustal and lithospheric scale based on these data and the 3D model of Klitzke et al. (2015). The transects, which extend onshore from the deep oceanic basins (Fig. 2), are used to link deep and shallow structures and processes, as well as to link offshore and onshore areas. From joint work carried out within three sectors (E, F & G; Fig. 1) of the Circum-Arctic Lithosphere Evolution (CALE) project we present regional profiles crossing all major geological provinces. Basin architecture and sedimentary deposits (stratigraphy) are linked to the structural evolution of the underlying crystalline crust and mantle lithosphere in these profiles. From field studies we integrate detailed information about structures, rock composition and age, and timing of tectonic events.

Regional setting and geological framework

The study area covers the Barents-Kara Shelf, which is bounded by Cenozoic passive continental margins towards the oceanic Norwegian-Greenland Sea in the west and the Eurasia Basin in the north (Figs. 1 & 2). The continental crust of the shelf and continental margins records several orogenic cycles, and the main geological events related to these addressed in this paper include: (1) Timanian orogeny; (2) Breakup/opening of the Iapetus Ocean; (3) Closure of the Iapetus Ocean – Caledonian Orogeny; (4) Opening of the Uralian Ocean; (5) Closure of the Uralian Ocean – Polar Urals, and Taimyr (two phases); and (6) Breakup/opening of the NE Atlantic (Norwegian-Greenland Sea) and Arctic Eurasia Basin.

The study area has also been affected by at least three episodes of regional-scale magmatism, resulting in formation of so-called large igneous provinces (LIPs): (1) Siberian Traps (latest Permian-earliest Triassic); (2) High Arctic Large Igneous Province (HALIP, Early Cretaceous); (3) North Atlantic (Paleocene-Eocene transition). In addition to these, Devonian mafic magmatism preserved in the Northern Timan-Kanin region is inferred to be related either to Devonian rifting (e.g., Pease et al., 2016) or Devonian LIP magmatism (Puchkov et al., 2016). Extensive magmatism in the Late Cretaceous centred on the Alpha Ridge area is included in the HALIP by some authors or is treated as a separate period of igneous activity post-dating continental breakup (Tegner et al., 2011). Regional uplift and subsidence associated with LIP magmatism can generate large-scale source-to-sink systems (e.g., Saunders et al., 2007).

The location of our lithosphere-scale transects with respect to gravity and magnetic anomalies are shown in figure 3. The free-air gravity field (Fig. 3a) is rather smooth across the Barents-Kara Sea showing that the shelf areas are in isostatic equilibrium. Prominent positive anomalies along the western and northern continental margins (Fig. 3a) are associated with depocenters of sediments deposited during the last 2-3 m.y. in front of bathymetric troughs formed by glacial erosion (Faleide et al., 1996; Dimakis et al., 1998; Vogt et al., 1998; Andreassen & Winsborrow, 2009; Laberg et al., 2012; Minakov et al., 2012a). The present plate boundary along the spreading system extending from the Norwegian-Greenland Sea and into the Arctic Eurasia Basin is clearly reflected in the free-air gravity anomaly map (Fig. 3a). The magnetic anomaly map (Fig. 3b) shows the characteristic linear sea-floor spreading anomalies of oceanic basins (Engen et al., 2008; Gaina et al., 2009; Jokat et al., 2016). In the continental part magnetic anomalies reflect a heterogeneous basement both onshore and offshore (Barrére et al., 2009, 2011; Marello et al., 2010, 2013; Gernigon & Brönner, 2012; Ritzmann & Faleide, 2007). Prominent magnetic anomalies at the northern Barents Sea margin, including eastern Svalbard and Franz Josef Land are associated with igneous rock intruded and extruded during Early Cretaceous magmatism (Polteau et al., 2016; Minakov et al., 2012b).

The most prominent feature in the depth to basement map (Fig. 4a) is the wide and deep East Barents Basin. This basin contains sedimentary fill up to 16-18 km thick (Roslov et al., 2009; Ivanova et al., 2011; Sakoulina et al., 2015, 2016). Deep sedimentary basins also exist in the SW Barents Sea, but these are much narrower and related to multiphase rifting (Faleide et al., 1993a,b; Gudlaugsson et al., 1998). The 3D model covers a wide range of basement provinces (Fig. 4b): (1) Cenozoic oceanic basement (Norwegian-Greenland Sea and Eurasia Basin); (2) Polar Urals – Novaya Zemlya – Taimyr; (3) Caledonian-Ellesmerian (North Greenland); (4) Caledonian (northern Norway-western Barents Sea-Svalbard; (5) Timanian; (6) Baltic Shield.

The depth to Moho map (Fig. 5a) clearly reflects the continent-ocean transition along the western (Faleide et al., 2008) and northern (Minakov et al., 2012a) margins. Moho depths are typically 30-35 km across the Barents-Kara Shelf, increasing to >40 km beneath the Baltic Shield in the south and the onshore orogenic belts in the east. The depth to the lithosphere-asthenosphere boundary (LAB; Fig. 5b) is based on shear wave velocity models from surface wave tomography (Levshin et al., 2007; Klitzke et al., 2015). It is shallow in the oceanic domain and adjacent parts of the continental margins. The central Barents Sea is characterized by intermediate depths while the LAB deepens significantly further east.

Transect selection and construction

The following criteria were used for selection of our regional transects: (1) Availability of deep seismic reflection and/or refraction data to constrain crustal structure; (2) location relative to main crustal domain boundaries (basement provinces, orogenic belts, sutures, etc.); (3) location relative to main structural elements; (4) potential for offshore-onshore correlations to areas where we have obtained new detailed information from CALE-related field work.

The first-order crustal and lithospheric structure along the regional transects were extracted from the 3D model of Klitzke et al. (2015) and displayed at two different vertical scales but the same horizontal scale. The crustal-scale section was then refined based on geophysical and geological data along the profiles, including (1) basin architecture (structure and stratigraphy), (2) depth to the top of the crystalline basement, (3) depth to Moho and (4) crustal heterogeneities (crustal-scale faults/shear zones). The sedimentary part is mainly based on multichannel seismic reflection data tied to wells; the crystalline part is based on P-wave velocity and gravity modeling; the mantle part is based on (isotropic) S-wave velocity model obtained by Levshin et al. (2007) using a surface wave tomography method.

Based on the criteria described above, we define the following six regional transects (see Figs. 2-5 for locations):

- Transect 1 - Norwegian-Greenland Sea to Pai Khoi (Fig. 6)
- Transect 2 - Norwegian-Greenland Sea to southern Kara Sea (Fig. 7)
- Transect 3 - Norwegian-Greenland Sea to Taimyr (Fig. 8)
- Transect 4 - Mezen Bay/Kanin Peninsula to Severnaya Zemlya (Fig. 9)
- Transect 5 - Baltic Shield/Fennoscandia to Eurasia Basin (Fig. 10)
- Transect 6 - Northern Norway (Troms) to Morris Jessup Rise (Fig. 11)

Table 1 summarizes the key references and main data sources used for the construction of the refined crustal-scale sections along these transects. These transects are described and discussed below.

Table 1 Principal references and data sources

Transect	Area	Key references
Transect 1	Norwegian-Greenland Sea - SW Barents Sea	Clark et al. (2013, 2014)
	Central and Eastern Barents Sea	Johansen et al. (1993)
	Pechora Basin – Pai Khoi	Sobornov (2013, 2015)
Transect 2	Norwegian-Greenland Sea – W Barents Sea	Breivik et al. (2003, 2005)
	E Barents Sea – Novaya Zemlya – S Kara Sea	Ivanova et al. (2011)
Transect 3	Norwegian-Greenland Sea	Ljones et al. (2004)
	Svalbard	Czuba et al. (2008)
	NW Barents Sea	Minakov et al. (2012b)
	N Barents Sea	Minakov et al. (*this volume*)
	NE Barents Sea – N Kara Sea	Ivanova et al. (2011)
	Taimyr	Afanasenkov et al. (2016)
Transect 4	Mezen Bay/Kanin Peninsula – Severnya Zemlya	Ivanova et al. (2011)
Transect 5	Onshore Fennoscandia	Lousto et al. (1989)
	S Barents Sea	Ivanova et al. (2011)
	Central Barents Sea	Khutorskoi et al. (2008)
	N Barents Sea – Eurasia Basin	Minakov et al. (2012a)
Transect 6	Northern Norway (Troms)	Indrevær et al. (2013)
	W Barents Sea – Svalbard	Jackson et al. (1993)
	Svalbard – Yermak Plateau – Morris Jessup Rise	Jokat et al. (1995)
		Geissler et al. (2011)

Results

For each transect we describe the (1) regional setting and location, (2) main crustal-scale structures and basin architecture, (3) deep lithosphere-scale structure and links to shallow structures/processes, and (4) offshore-onshore links. These transects, together with the maps from the 3D model introduced above (Figs. 2-5), form the basis for the discussion that follows and addresses the regional geological evolution with focus on orogenesis and basin development.

Transect 1

Transect 1 (Fig. 6) extends from the Norwegian-Greenland Sea in the west, across the southern Barents Sea to the Pechora Basin and onshore Pai Khoi in the east (see Figs. 2-5 for location and Table 1 for references).

In the oceanic domain the transect crosses the plate boundary at the transition from the Mohns Ridge to the Knipovich Ridge. The oceanic basin is filled with a thick succession of Eocene and younger sediments. More than half the volume of this forms a wedge of prograding glacial sediments deposited during the last 2-3 million years (Faleide et al., 1996; Laberg et al., 2012). The continent-ocean transition (COT) is sharp at the mainly sheared SW Barents Sea margin (Faleide et al., 2008). Landward of the COT the Vestbakken Volcanic Province (VVP) reveals that early Cenozoic breakup was associated with volcanic activity as seen on most NE Atlantic margins. VVP is located at a predominantly rifted margin segment which linked sheared margin segments to the south and north. Repeated tectonic and volcanic activity within the VVP indicates a more complex Cenozoic evolution for the Greenland Sea than is indicated by the traditional two-stage evolutionary model (e.g., Engen et al., 2008), and as much as 8 tectonic and 3 volcanic events have been identified (Faleide et al., 2008).

The Bjørnøya Basin is one of the deep and narrow basins in the SW Barents Sea that formed in response to several rift phases affecting the NE Atlantic region from Late Paleozoic time to final continental breakup at the Paleocene-Eocene transition (Faleide et al., 1993a,b). The main rift phases have been dated to Carboniferous, Late Permian, Late Jurassic-Early Cretaceous and Late Cretaceous-Paleocene (Faleide et al., 2008, 2015; Tsikalas et al., 2012). These multiple stretching events resulted in a thinned crystalline crust under the deep basins (Faleide et al., 2008; Clark et al., 2013). The crust, and also the lithospheric mantle, is significantly thicker under the platform area to the east, which has not seen rifting since the Carboniferous (Fig. 6). The basins formed during the Carboniferous rift event (e.g., Nordkapp Basin) were filled with thick evaporite deposits that later were mobilized as salt diapirs (Faleide et al., 2015). The transition between Caledonian basement in the west and Timanian basement in the east is located within the platform area east of the main rift basins (Ritzmann & Faleide, 2007, 2009; Gernigon & Brönner, 2012; Gernigon et al., 2014).

The East Barents Basin is very different from the Carboniferous rift basins in the SW Barents Sea. It has a width of 400-600 km and extends for more than 1000 km in the N-S direction (Figs. 4a & 6). Very thick basin fill reflects significant subsidence but there are no signs of major faulting associated with the main phase of subsidence in the late Permian-earliest Triassic (Johansen et al., 1993; Ivanova et al., 2011). Beneath the flanks of the East Barents Basin there are faults indicating Late Devonian rifting but it is not likely that this rifting was the direct cause of the rapid regional subsidence that occurred 100 m.y. later over the entire eastern Barents Sea. Gac et al. (2012, 2013) tested various mechanisms for the basin's formation and preferred a model involving phase changes at depth, in the lowermost crust/uppermost mantle. The crystalline crust under the East Barents Basin is relatively thick so the basin appears to be isostatically compensated by a high-density body around the crust-mantle transition rather than by crustal thinning (Klitzke et al., 2015). This high-density body could have been emplaced in response to crustal thinning-decompression melting in relation to the Late Devonian rifting. If this melt was trapped at the base of the crust, it would have slowly cooled and caused long-term subsidence without significant faulting. The presence and nature of this body will be further discussed in relation to Transect 2.

Sill intrusions related to Early Cretaceous magmatism (HALIP) are widespread in the East Barents Basin, making imaging of the deep basin configuration difficult (e.g., Polteau et al., 2016). The profile reaches the onshore area in the northern Pechora Basin adjacent to the

Pai Khoi fold belt, not far away from the northern end of the Polar Urals. Here, a thick foreland basin fill is associated with uplift of the fold-and-thrust belt in Late Triassic time (Sobornov, 2015).

Transect 1 links to onshore field studies in the Pai Khoi region where structural evidence indicates that the NW-SE trending fold belt in southernmost Novaya Zemlya may have formed contemporaneously with early Mesozoic sinistral strike-slip faulting (Curtis et al., *this volume*). Structural data from the Main Pai Khoi Thrust documents an oblique tectonic stretching lineation, consistent with tectonic displacement toward the west. Large-scale structural relationships are also consistent with sinistral shear along the Pai Khoi fold and thrust belt (PKFB) and include left stepping en-echelon folds. Therefore, the deformation within the PKFB is best described as sinistral transpression, which has implications for the interpretation of this tectonic boundary within Transect 1. Fission track data further clarify the tectonic evolution of this region. Zircon fission track (ZFT) analyses indicate that Silurian to early Permian strata across Novaya Zemlya have never been at temperatures higher than 250°C. Apatite fission-track ages from the same study define a period of rapid exhumation and cooling to below c. 100°C at 220-210 Ma across the archipelago (Zhang et al., a *this volume*). Consistent with these new observations (Curtis et al., *this volume*; Zhang et al., a *this volume*), we interpret the eastern end of Transect 1 to have been affected by Triassic thick-skinned folding and thrusting. This is also consistent with the thickened crust and lithosphere seen in Transect 1 (Fig. 6).

The lithosphere-scale structure along Transect 1 (Fig. 6) shows a deepening of the LAB from west to east (Klitzke et al., 2015). The oceanic domain and adjacent parts of the margin are underlain by thin (~50 km) lithosphere. The mantle below has slow shear wave velocities (Levshin et al., 2007), likely indicating elevated mantle temperatures (Klitzke et al., 2016). Mantle tomography indicates a braided pattern of large low-velocities anomalies in the North Atlantic upper mantle extending to the northwest Barents Sea margin (e.g., Rickers et al., 2013). The lithosphere in the western Barents Sea has an intermediate thickness of typically 100 km before it thickens significantly in the eastern Barents Sea. From Novaya Zemlya and eastward to the mainland of Russia, the lithosphere is about 200 km thick. The eastward thickening of the lithosphere also reflects an increase in strength (Gac et al., 2016;

Klitzke et al., 2016) which impacts the tectonic/structural evolution of the area by focusing deformation at its thinner/weaker margins.

Transect 2

Transect 2 (Fig. 7) extends from the Norwegian-Greenland Sea in the west, across the central Barents Sea, Novaya Zemlya and the Kara Sea to onshore parts of the West Siberian Basin in the east (see Figs. 2-5 for location and Table 1 for references).

In the oceanic domain Transect 2 crosses the plate boundary at the Knipovich Ridge. A thick succession of Cenozoic sediments occupies the area between the ridge and outer parts of the Barents Shelf (Faleide et al., 1996; Hjelstuen et al., 1996). The continent-ocean transition (COT) is sharp at the mainly sheared western Barents Sea margin (Breivik et al., 2003; Faleide et al., 2008). The base of the crust deepens from <10 km to >30 km over a narrow zone of about 50 km. Landward of the COT the profile rapidly reaches the wide Svalbard Platform which has seen no rifting since Late Paleozoic times (Faleide et al., 1984). The deep seismic data, both reflection and refraction, reveal a characteristic basement terrane in western parts of the platform which is interpreted to represent Caledonian basement (Gudlaugsson et al., 1987; Gudlaugsson & Faleide, 1994; Breivik et al., 2003). Two branches of Caledonian basement have been proposed, one extending N-S towards Svalbard and the other having a NNE trend up through the northern Barents Sea between Svalbard and Franz Josef Land (Gudlaugsson et al., 1998; Breivik et al., 2005; Ritzmann & Faleide, 2007; Marello et al., 2013; Knudsen et al., *this volume*).

Transect 2 crosses central parts of the wide and deep East Barents Basin (profile distance 1000-1500 km; Fig. 7), as previously described along Transect 1 above (Fig. 6). A high-velocity body around the crust-mantle transition beneath the deepest part of the basin was suggested by Ivanova et al. (2011) but an alternative interpretation of the same seismic refraction profile was published by Roslov et al. (2009).

West of Novaya Zemlya we see evidence of the final upthrusting of Novaya Zemlya and a Late Triassic (-?Early Jurassic) age has been suggested for this (Zonenshain et al., 1990;

Bogatsky et al., 1996; Ritzmann & Faleide, 2009). Here, Jurassic strata is separated from deformed Middle-Upper Triassic strata by an angular unconformity (Khlebnikov et al., 2011; Artyushkov et al., 2014; Nikishin et al., 2014, Shipilov, 2015). Crustal thickening and uplift is associated with the fold belt (Fig. 7) and the Late Triassic timing of exhumation is consistent with structural observations from southernmost Novaya Zemlya (Curtis et al., *this volume*) and apatite fission track cooling ages across Novaya Zemlya (Zhang et al., *this volume*). The eastern Barents Sea received considerable thicknesses of Lower-Middle Jurassic sediments derived from uplifted Novaya Zemlya (Suslova, 2014).

The South Kara Sea east of Novaya Zemlya forms the westernmost part of the large West Siberian Basin. The nature of the basement and deep basin configuration is poorly constrained by the available data. A rather thick Mesozoic basin fill is underlain by faulted structures of assumed Late Permian-Triassic age (Nikishin et al., 2011). The western flank of the South Kara Basin, towards Novaya Zemlya, indicates thick Paleozoic strata deformed during Permo-Triassic uplift of the fold belt (Fig. 7). Onshore, in the south island penetrative cleavage development is only present in Silurian and older units (Pease, unpublished data), while younger strike-slip faulting cuts all units (Curtis et al., *this volume)*. On the north island, however, penetrative deformation affects all units and is at least Late Triassic in age. Consequently we presume that a Paleozoic event and a brittle younger Late Triassic event can be seen in southern Novaya Zemlya, while in the north Triassic deformation is strong, pervasive, and occurred under ductile conditions. Paleozoic deformation may have been localized in the south, or Mesozoic deformation fully overprinted Paleozoic deformation in the north. Judging from the offshore record, the younger deformation is the principle compressive event in the central and northern parts of the archipelago.

The lithosphere-scale structure along Transect 2 (Fig. 7) has many similarities to Transect 1 (Fig. 6) further south, reflecting the systematic deepening of the LAB from west to east (Levshin et al., 2007; Klitzke et al., 2015). Thin lithosphere underlain by a low-velocity, hot mantle in the west (Klitzke et al., 2016) is even more prominent in Transect 2. The low-velocity anomaly in the South Kara Sea region may indicate a younger thermal age of the lithosphere here. However, the interpretation in the uppermost mantle is complicated by trade-offs with poorly constrained crustal velocities.

Transect 3

Transect 3 (Fig. 8) extends from the Norwegian-Greenland Sea in the west, across Svalbard and the northern Barents-Kara Sea to onshore Taimyr in the east (see Figs. 2-5 for location and Table 1 for references).

In the oceanic domain Transect 3 crosses the plate boundary at the Knipovich Ridge. The continent-ocean transition (at profile distance ~350 km) is sharp across the first sheared and later obliquely extended western Svalbard margin (Faleide et al., 2008; Krysinski et al., 2013; Grad et al., 2015). In western Spitsbergen it crosses the Paleogene (mainly Eocene) Spitsbergen fold-and-thrust belt and the associated foreland basin (Bergh et al., 1997; Braathen et al., 1999; Leever et al., 2011; Blinova et al., 2013). This contractional event was linked, both in time and space, to Eurekan deformation in Ellesmere Island and North Greenland (Piepjohn et al., 2016; Piepjohn & von Gosen, *this volume*). The remaining part of Svalbard and adjacent area of the northern Barents Sea belong to the same wide platform described for Transects 1 & 2. It is also underlain by Caledonian basement. Early Cretaceous igneous extrusives and intrusives are known both from onshore Svalbard and adjacent offshore areas (Grogan et al., 2000; Minakov et al., 2012b). A northward continuation of the Caledonian deformation front seen in Transect 2 was proposed by Marello et al. (2013) on the basis of their combined 3D gravity and magnetic model. This basement boundary passes west of Franz Josef Land and is consistent with the presence of Timanian basement at depth (>2 km) in the Nagurskaya borehole on Alexandra Land, Franz Josef Land (Dibner, 1998; Pease et al., 2001).

Transect 3 crosses the northernmost parts of the wide and deep East Barents Basin (profile distance 1000-1500 km), as already described along Transects 1 and 2. Igneous intrusions, both sills and dykes as known from outcrops on adjacent Franz Josef Land, are well imaged by seismic reflection data. The deep seismic refraction data indicate crustal heterogeneities, high-velocity zones likely representing remnants of feeder systems for shallow intrusive and extrusive rocks (Minakov et al., *this volume*).

The northern Kara Sea is distinctly different from both the northern Barents Sea and the southern Kara Sea in terms of basement structure and sedimentary infill (Fig. 8; Profile distance 1900-2200 km). The mantle lithosphere of the northern Kara Sea is characterized by higher shear velocities (4.6-4.7 km/s) compared to Transect 2 in the south (4.4-4.6 km/s). A thin cover of upper Paleozoic?-Mesozoic strata is underlain by assumed thick lower Paleozoic strata (including salt/evaporites) and a basement of Timanian age (Malyshev et al., 2012a, 2012b). Approaching Taimyr the profile crosses major faults which are likely linked to the folding and thrusting seen onshore.

Onshore field studies carried out in eastern Taimyr (Zhang et al., b *this volume*) provide important data that help to interpret seismic data offshore along Transect 3. The late Paleozoic (Uralian) collision across Taimyr resulted in thrusting of Paleozoic rocks in central Taimyr and the deposition of syn-tectonic siliciclastic successions in the foreland basin of southeastern Taimyr (X. Zhang et al., 2013, 2015, 2016). The southward-propagating thrust system has both thin- and thick-skinned deformation that dips to the north (e.g., Lacombe & Bellahsen, 2016) (Fig. 8). A similar structural style but with northward vergence has been interpreted as the conjugate side of the bivergent Uralian orogen north of Taimyr (e.g., Malyshev et al., 2012a). Combined balanced cross-sections and apatite fission track analyses (Zhang et al*., b this volume*) recognize three cooling episodes across Taimyr: (1) Early Permian, (2) earliest Triassic, and (3) Late Triassic. These authors interpret the cooling events to indicate uplift associated with thickening during early Permian (Uralian) convergence, followed by later heating, uplift, and cooling associated with Siberian Trap magmatism (crustal thinning?) and/or Mesozoic transpression. In central and eastern, Taimyr Zhang et al. (*b this volume*) estimate 15% shortening due to Uralian compression across the Uralian foreland of southern Taimyr. Thick-skinned thrusting requires that this shortening is a minimum. The regional structures continue across to western Taimyr. We infer that Uralian orogenesis was also in part responsible for the thickened crust and lithosphere seen here (Fig. 8). The suture exposed at the surface between crust of inferred Baltican affinity to the north and Siberian affinity to the south (see Pease & Scott, 2009) is seen in the structure of the lower crust and lithospheric mantle in western Taimyr (at c. 2200-2300 km in Fig. 8). This implies that the lithosphere is stable and still preserves its older structure.

In general, the lithosphere-scale structure along Transect 3 shows many similarities to Transects 1 and 2 further south, such as the systematic deepening of the LAB from west to east and a thin lithosphere underlain by slow/hot mantle in the west. Thin lithosphere under Spitsbergen has been inferred from xenoliths sampled in lavas from a Quaternary volcano in northern Spitsbergen (Vågnes & Amundsen, 1993). Volcanic activity since Miocene time (10 Ma; Prestvik, 1978) and high temperature gradients of 40-50 deg/km (Marshall et al., 2015) can be related to the anomalous lithospheric structure observed in this area (Fig. 8) and will have influenced the recent history of uplift and erosion. The shallow geothermal gradient may be elevated due to radioactive heat generation in the crust and lower thermal conductivity of crustal rocks compared to mantle rocks and thus not directly representative of the mantle geothermal gradient.

Transect 4

Transect 4 (Fig. 9) extends from Severnaya Zemlya at the northern margin of the Kara Sea, across the Kara and Pechora seas, to the Mezen Bay/Kanin Peninsula in the south (see Figs. 2-5 for location and Table 1 for references).

The northern Kara Sea (also covered by Transect 3; Fig. 8) has a thick lower Paleozoic sedimentary succession deposited on presumed Timanian basement, later deformed by late Paleozoic contraction and covered by a thin Mesozoic unit (Malyshev et al., 2012a, 2012b). This evolution is probably over-simplified given the geology exposed on Severnaya Zemlya where the Paleozoic section includes unconformities and disconformities. In addition, numerous décollements associated with latest Devonian to earliest Carboniferous folding and thrusting are well-documented (see Lorenz et al., 2007, 2008 and references therein). Nonetheless, basal strata are Neoproterozoic in age and on the basis of geophysical data we presume Neoproterozoic (Timanian?) basement also occurs offshore.

The South Kara Basin in the central part of the profile (Fig. 9), also covered by Transect 2 (Fig. 7), is bounded by prominent structures both in the south and north. The southern boundary, in the Kara Strait between Novaya Zemlya and Vaygach Island, is inferred to be a NW-SE trending zone of sinistral transpression extending from Pai Khoi (eastern end of Transect 1;

Fig. 6) to Novaya Zemlya (Curtis et al., *this volume*). The final phase of deformation associated with this structure is Late Triassic in age (see Curtis et al., *this volume*; Zhang et al., *a this volume*).

The northern boundary of the South Kara Basin is defined offshore by the North Siberian Arch (Malyshev et al., 2012a), which separates the southern and northern Kara seas (Figs. 4 & 9). Onshore, the northern boundary of Novaya Zemlya has been suggested to be a dextral strike-slip fault which geometrically accommodates the Novaya Zemlya salient (Otto & Bailey, 1995). However, there is no evidence for dextral strike-slip faulting on the north island of Novaya Zemlya (see also Scott et al., 2010). The North Siberian Arch is an older feature that was later uplifted in Late Triassic (-?Early Jurassic) times (Malyshev et al., 2012a); it presumably links Mesozoic deformation between northern Novaya Zemlya and Taimyr where Triassic E-W dextral strike-slip faulting is well-documented (Inger et al., 1999). In northern Taimyr, Cambrian metasediments were structurally emplaced during collision between Baltica and Siberia at 304 Ma, which is interpreted to represent the continuation of Uralian deformation in the Arctic (Pease & Scott, 2009; Pease et al., 2015). Seismic data from the Yenisei Bay towards the Kara Sea (Stoupakova et al., 2012, 2013) show evidence of two contractional events, one affecting lower Permian and older strata and a younger one also involving upper Permian-Triassic strata. The driving mechanism for Mesozoic deformation across Taimyr and Novaya Zemlya is unknown and a major problem for understanding the tectonic evolution of the region. Drachev (2016) speculated that it may be related to a northern push of the Siberian Craton as a part of Laurasia via collision, with the Cimmeria continent at end-Triassic time.

The southern part of Transect 4 crosses the offshore part of the Pechora Basin which is known to be underlain by Timanian basement. This basement is partly exposed onshore (Lorenz et al., 2004; Pease et al., 2014 and references therein). All of Transect 4 is underlain by a thick, strong lithosphere. Typical depths to the LAB range between 150 and 200 km (Fig. 9). The crustal thickness is 35-40 km except in central parts of the southern Kara Sea where it is slightly thinner (30-35 km).

Transect 5

Transect 5 (Fig. 10) extends from the Eurasia Basin in the north, across the entire Barents Sea to the Baltic Shield/Fennoscandia in the south (see Figs. 2-5 for location and Table 1 for references).

In the oceanic domain the transect crosses the plate boundary at the ultra-slow spreading Gakkel Ridge (e.g., Vogt et al., 1979, Dick et al., 2003). The Cenozoic Nansen Basin is filled with a thick sedimentary succession mostly derived from the uplifted Barents Shelf (Jokat & Micksch, 2004; Geissler & Jokat, 2004; Engen et al., 2009; Berglar et al., 2016). A significant part of this basin fill consists of sedimentary fans deposited in front of major bathymetric troughs crossing the northern Barents Sea margin similar to what is seen along the western Barents Sea margin (Faleide et al., 1996; Minakov et al., 2012a). The continent-ocean transition (COT) is sharp at the northern Barents Sea margin, where the base of the crust deepens from <10 km to >30 km over a narrow zone. This crustal architecture led Minakov et al. (2012a, 2013) to propose a phase of short-lived shear during initial breakup before the Lomonosov Ridge separated from the northern Barents Shelf by seafloor spreading. Across the entire Barents Shelf the depth to Moho is typically 30-35 km.

The Central Barents Sea contains a number of structural highs (Khutorskoi et al., 2008), which are not well understood because of limited seismic data and a lack of boreholes. Some of the highs show evidence of at least two phases of uplift. The last phase of uplift post-dates Cretaceous strata subcropping at the seafloor (Fig. 10). Some of these highs are late Paleozoic features, but others, at least in part, represent inverted basins. These structural highs have different signatures in potential field (gravity and magnetic) data, which may reflect both a heterogeneous basement and elements of basin inversion.

The crustal-scale boundary between the presumed Caledonian and Timanian basement provinces is crossed in the central Barents Sea (Fig. 4). The profile also crosses the Trollfjord-Komagelva Fault (TKF), another long-lived fundamental boundary which extends c. 1800 km from near the Varanger Peninsula of the Norwegian Mainland to the northern Kola coast of NW Russia, and beyond that to the Timanides (Olovyanishnikov et al., 2000). In the late

Neoproterozoic the TKF was a major normal fault separating a pericratonic fluvial to shallow-marine domain from a more outboard, deltaic to deeper marine, basinal domain (see W. Zhang et al., 2016 and references therein). This structure was reactivated during Caledonian deformation in latest Cambrian to early Ordovician time when a part(s) of the Barents shelf was dextrally displaced >200 km to its present position (W. Zhang et al., 2016 and references therein). Along Transect 5 (Fig. 10), the area immediately north of this fault is today characterized by thick metasediments that were intruded by massive dykes of Devonian age (Guise & Roberts, 2002). South of the fault, a crustal thickness of >40 km is observed, consistent with a stable shield terrane.

Across the Barents Shelf, Transect 5 is located within the province of intermediate lithospheric thickness (typically 100 km). The lithosphere thins significantly towards the oceanic domain in the north and thickens towards the shield area in the south (Fig. 10).

Transect 6

Transect 6 (Fig. 11) extends from the Morris Jessup Rise in the north, across the Eurasia Basin to the Yermak Plateau, and through the western Barents Sea from Svalbard to Mainland Norway (Troms) in the south (see Figs. 2-5 for location and Table 1 for references).

The western Eurasia Basin is bounded by the conjugate Morris Jessup Rise and Yermak Plateau. There, the crustal structure and composition of these features are poorly constrained, but believed to be at least partly of continental origin with some volcanic overprint (Geissler et al., 2011; Jokat et al., 2016). This provides challenges for plate reconstructions back to the time of breakup since the Morris Jessup Rise and Yermak Plateau start to overlap at magnetic chron 13 in the early Oligocene (Engen et al., 2008).

The profile runs through Svalbard parallel to the main N-S trending faults that separate crustal blocks (Billefjorden and Lomfjorden fault zones; Dallmann, 2015). Between Svalbard and Bjørnøya the profile extends along the western flank of the Svalbard Platform which is a late Paleozoic paleo-high (Anell et al., 2016). It is underlain by Caledonian basement as described for the crossing Transect 2 (Fig. 7). Transect 6 also runs through Bjørnøya, which offers insights into the geology of the western Barents Sea (Worsley et al., 2001).

South of Bjørnøya and the surrounding Stappen High, the profile crosses the deep sedimentary basins of the SW Barents Sea (Faleide et al., 1993a,b), also crossed by Transect 1 (Fig. 6). The southern flank of the Stappen High towards the deep Bjørnøya Basin was inverted in early Cenozoic time (Blaich et al., 2012, 2017). The basin province in the south has a much thinner crystalline crust than the platform area in the north (Fig. 11). Numerous salt diapirs are found throughout the deep basins of the SW Barents Sea, in particular in the Tromsø Basin. These evaporites were deposited around the Carboniferous-Permian transition in a regional basin extending from the Central Barents Sea to offshore NE Greenland (Faleide et al., 1993a, 2015). Transect 1 ends onshore in Troms, northern Norway (Indrevær et al., 2013, 2014). This part of the transect is underlain by Caledonian basement (Fig. 4; Ritzmann & Faleide, 2007; Gernigon & Brönner, 2012). The lithosphere is very thin from the Stappen High and northwards to Svalbard, within an area that was affected by significant Neogene uplift (Dimakis et al., 1998; Henriksen et al., 2011b). In the south the lithosphere thickens beneath the deep basins towards the mainland where a dramatic step in the LAB is also seen (Fig. 11).

Discussion

The regional geological evolution of the wider Barents-Kara Sea region is summarized and discussed with reference to the regional transects (Figs. 6-11) and maps (Figs. 2-5). We integrate detailed information from onshore field studies and other complementary studies, mainly based on seismic and well data. In addition, a tectono-stratigraphic summary highlights the main regional events (Table 2). This discussion is divided into two parts. The first part addresses the orogens that have affected the study area. For each of these we summarize and discuss the main observations, extent, timing, structural style and driving force(s). The second part focuses on basin development. For each of the regional tectonic events and stages in basin evolution we summarize and discuss timing, causes and implications. Fault activity is related to regional stress regimes and the role of inheritance (reactivation of pre-existing basement/structural grain). Regional uplift/subsidence events are discussed in a source-to-sink context and related to their regional tectonic and paleogeographic settings.

Orogenesis

The study area has been affected by numerous orogenic events: (1) Precambrian-Cambrian (Timanian); (2) Silurian-Devonian (Caledonian); (3) Latest Devonian-earliest Carboniferous (Ellesmerian/Svalbardian); (4) Carboniferous-Permian (Uralian); (5) Late Triassic (Taimyr, Pai Khoi, Novaya Zemlya); (6) Paleogene (Spitsbergen/Eurekan).

Precambrian-Cambrian (Timanian Orogen)

The Timanide Orogen can be followed for 2000 km from the southern Polar Urals to the Varanger Peninsula in northern Norway, where it is truncated by later Caledonian deformation (Fig. 4; Pease et al., 2014 and references therein). Timanian orogenesis (sensu stricto) post-dates alkaline magmatism documenting extension at c. 610 Ma (Larianov et al., 2004) and the accretion of island arc and marginal sediments as young as Cambrian in age (Pease & Scott, 2009). The north-westerly strike of this 'basement' onshore, its presence at >2 km depths in drillcore from Franz Josef Land (Dibner, 1998; Pease et al., 2001), and geophysical data offshore (Ritzmann & Faleide, 2009; Ritzmann et al., 2007; Gernigon & Brönner, 2012; Marello et al., 2010, 2013) indicates that Timanian basement extends from the onshore Pechora Basin (Transect 1; Fig. 6) across the eastern/central Barents Sea (albeit deeply buried) (Fig. 4). Similar rocks present in northern Taimyr and on southern Severnaya Zemlya (Lorenz et al., 2007) suggest that Timanian basement is also present at depth beneath the north Kara Sea (Transects 3 & 4; Figs. 8 & 9) (Pease & Scott, 2009; Malyshev et al., 2012a,b).

Silurian-Devonian (Caledonian Orogen)

Most of the western Barents Sea is underlain by basement affected by Caledonian deformation but there are uncertainties about the eastern limit of the Caledonian suture and deformation front (e.g. Gudlaugsson et al. 1998; Gee et al., 2006; Barrére et al., 2009; Henriksen et al., 2011a; Pease, 2011; Pease et al., 2014). Caledonian rocks are known from

NE Svalbard (Nordaustlandet) and Kvitøya (Johansson et al., 2005), but are absent from Franz Josef Land (Dibner, 1998; Pease et al., 2001). Magnetic data indicate that the main Caledonian structures turn to a NNW orientation just off the coast of northern Norway and continue northwards to Svalbard (Gernigon & Brönner, 2012). This is further supported by deep seismic reflection and refraction data (Gudlaugsson et al., 1987, 1998; Gudlaugsson & Faleide, 1994; Breivik et al., 2005; Ritzmann & Faleide, 2007). However, a second Caledonian branch trending SW-NE in the northern Barents Sea between Svalbard and Franz Josef Land has been postulated from deep seismic data (Breivik et al., 2002) and potential field (magnetic and gravity) anomalies (Marello et al., 2010, 2013). Hints of Caledonian thermal re-working have recently been reported from the Lomonosov Ridge, where white mica defining the foliation in two dredge samples yield broadly Caledonian ^{40}Ar/^{39}Ar ages (Knudsen et al., *this volume*). The nature of this basement terrane boundary is a subject of ongoing research (Aarseth et al., 2017).

Latest Devonian?-earliest Carboniferous (Svalbardian- Ellesmerian deformation)

Svalbardian-Ellesmerian deformation is seen as westward thrusting associated with generally east-west compression in the earliest Carboniferous (Tournaisian) (Piepjohn et al., 2000). The regional extent of Tournaisian folding and thrusting from NW Svalbard to the Ellesmerian fold belt of North Greenland and Ellesmere Island in the Canadian archipelago indicates its significance. The deformation style involved both thin- and thick-skinned thrusting and is apparently the result of interactions between Svalbard and north Greenland during earliest Carboniferous time (Piepjohn et al., 2000). The driving mechanism for Svalbardian-Ellesmerian deformation, however, is enigmatic.

Carboniferous-Permian (Uralian Orogen)

The Arctic continuation of the diachronous Uralian Orogen from the Polar Urals to Taimyr has been highly debated (see Pease, 2011 and Pease et al., 2014 and references therein). Paleozoic folding and thrusting and associated magmatism at 320-280 Ma in the Polar Urals and on Taimyr (Vernikovsky , 1995; Bea et al., 2002; Scarrow et al., 2002; Zhang et al., 2013, 2015,b 2016; Pease et al., 2015) document Uralian collision. Most workers link the Polar Urals via Novaya Zemlya to Taimyr, yet the evidence from Novaya Zemlya is ambiguous given the difference in style and timing of deformation discussed earlier. An early Permian cooling event in Taimyr is well-documented and has been linked to uplift associated with inferred Uralian aged convergence in the Arctic (Zhang et al., *b this volume*), but in Novaya Zemlya this event is not seen.

Late Triassic (Taimyr, Pai Khoi, Novaya Zemlya fold belts)

Seismic data adjacent to Pai Khoi and Novaya Zemlya indicate that Triassic strata were involved in contractional deformation (Stoupakova et al., 2011; Sobornov, 2013, 2015). In the eastern Barents Sea, in front of Novaya Zemlya, Jurassic strata overlay deformed Middle-Upper Triassic strata (Khlebnikov et al., 2011; Artyushkov et al., 2014; Nikishin et al., 2014, Shipilov, 2015). The timing of the final up-thrusting of Novaya Zemlya must be within this hiatus. This is consistent with new data from Novaya Zemlya that records Late Triassic uplift and exhumation across the whole of the island (Zhang et al., a *this volume*). Although the data is sparse, the Zhang study also suggests that exhumation may young to the NW in the direction of thrust propagation, supporting a younger age of deformation towards the foreland. This is consistent with hiatus across the angular unconformity in front of Novaya Zemlya described above, which appears to extend into the Jurassic. Similar to Novaya Zemlya, a Late Triassic uplift and cooling event is recorded across Taimyr, however Taimyr also preserves a well-documented record of Uralian age convergence, uplift, and exhumation (Zhang et al., 2013, 2015, b *this volume*). Scott et al. (2010) suggested that the absence of Carboniferous to Permian-age Uralian deformation on Novaya Zemlya was due to a natural embayment of the Baltica margin, an interpretation shared by Drachev et al. (2010). In this scenario Novaya Zemlya was protected within the embayment and distal to the Uralian deformation front. Further investigations into the timing and overprinting of deformation events in the area are needed.

Paleogene (Spitsbergen/Eurekan fold belts)

Eurekan deformation is related to circum-Greenland plate boundaries in early Cenozoic time (Piepjohn et al., 2016). The northward movement of Greenland resulted in compression and intra-plate contractional deformation on Ellesmere Island. Accordingly, the Eurekan foldbelt is linked through North Greenland to Spitsbergen which also shows the onset of compressional deformation and an associated shift in sediment provenance close to the Paleocene-Eocene transition (Petersen et al., 2016). The main phase of deformation occurred in the Eocene. In Spitsbergen this was associated with dextral strike-slip faults linking the early opening of the Norwegian-Greenland Sea with the Eurasia Basin (Faleide et al., 2008). Approximately 20–40 km margin-perpendicular shortening accumulated in the Spitsbergen fold-and-thrust belt. This has been attributed to transpression and strain partitioning in a strike-slip restraining bend located SW of Spitsbergen (Leever et al., 2011). Thin-skinned deformation occurred above a decollement in Permian gypsum and Mesozoic black shale, while thick-skinned shortening reactivated the pre-existing N-S trending older zones of weakness running through Svalbard (Bergh et al., 1997; Braathen et al., 1999).

Basin development

The study area is underlain by basement provinces of different ages as summarized above. The post-orogenic basin development starts at different times throughout the study area.

<u>Early Paleozoic</u>

Lower Paleozoic sedimentary strata are found in basins underlain by Timanian basement. This is best known from the Pechora Basin (Transects 1 & 4; Figs. 6 & 9) and northern Kara Sea (Transects 3 & 4; Figs. 8 & 9) where thick successions of assumed Cambrian to Silurian (?) age strata, including Ordovician salt, are found below a thin cover of Mesozoic strata (Maslov, 2004; Malyshev et al., 2012a, 2012b). Rocks of similar age are probably also present in other areas underlain by Timanian basement, such as in the eastern Barents Sea, but here they are buried much deeper due to formation of younger basins (in particular during Permian-Triassic times). Deep burial (compaction/metamorphism) has turned them into metasediments, which are difficult to image. Deep in the eastern flank of the East Barents Basin layered strata of likely Early Paleozoic age are observed (e.g., Transect 3; Fig. 8). At the southern flank, in the Varanger–Kola monocline, Early Paleozoic strata have also been interpreted (Transect 5; Fig. 10), consistent with the NW strike of structural fabrics onshore.

<u>Late Paleozoic</u>

The Late Paleozoic configuration of the western and central Barents Sea consists of three different generations of basin formation characterized by different size and orientation: (1) The oldest is interpreted to be of Devonian age and related to collapse of the Caledonian

Orogen, partly by extensional reactivation of the orogen's frontal thrusts. High-quality magnetic data show that these thrusts turn from a NE to NNW trend just off the coast of northern Norway (Gernigon & Brönner, 2012; Gernigon et al., 2014). Thick units of non-magnetic sediments were deposited in front of the orogen as reflected by deep seismic data (e.g., Transect 2; Fig. 7) (Gudlaugsson et al., 1987, 1994; Gudlaugsson & Faleide, 1994; Breivik et al., 2005; Ritzmann & Faleide, 2007) and estimated depths to magnetic basement (Gernigon & Brönner, 2012). In the SW Barents Sea one of these Devonian basins is informally named Scott Hansen complex by Gernigon & Brönner (2012). (2) The Carboniferous rift structures like the Nordkapp and Ottar basins (Transect 1; Fig. 6), on the other hand, are better revealed by seismic and gravity data (Breivik et al., 1995; Gudlaugsson et al., 1998). New high-quality long-offset seismic reflection data show a horst and graben basin relief with a dominant NE to NNE trend, which also gives rise to lateral density variations reflected by the gravity anomalies (Fig. 3a). In some areas these structures cut through the underlying structural grain while in other areas they seem to reactivate the pre-existing grain. It is not clear if these structures were linked to regional extension in the proto-Arctic and/or North Atlantic region. The Carboniferous horst and graben basin configuration in the western and central Barents Sea affected the depositional systems and facies distribution within the overlying Carboniferous-Permian succession which is dominated by carbonates and evaporites (see below; Gudlaugsson et al., 1998). The rift structures and associated evaporites also played a role in the later reactivation and formation of contractional structures. (3) New seismic reflection data also reveal evidence of an important late Permian rift phase mainly affecting the deep sedimentary basins of the SW Barents Sea (e.g. the Tromsø and Bjørnøya basins; Faleide et al., 2015), which were an integral part of a regional rift system within the North Atlantic region. This may be linked to the Sverdrup Basin in Arctic Canada through North Greenland and Ellesmere (Håkansson et al., 2015).

The eastern Barents Sea area, including the Pechora Basin, was affected by Late Devonian – ?early Carboniferous rifting and associated magmatism (Nikishin et al., 1996; Wilson et al., 1999; Petrov et al., 2008; Pease et al., 2016). Rift structures likely related to this phase are observed beneath the eastern flank of the deep East Barents Basin (e.g. Transects 1 & 2;

Figs. 6 & 7). Devonian dolerite dykes reported from the eastern Varanger Peninsula, North Norway (Guise & Roberts, 2002) have also been linked to rifting (Pease et al., 2016).

A wide part of the Arctic, including the Barents Sea, was covered by a late Carboniferous-early Permian carbonate platform deposited in a stable tectonic setting. Carbonate buildups (bioherms) developed along the flanks of underlying Late Paleozoic structural highs, and evaporites were deposited in basins coinciding with underlying Carboniferous rifts (Larssen et al., 2005).

Rapid latest Permian-earliest Triassic subsidence affected most of the Barents Sea area, and large volumes of sediments sourced from southeast (Urals) and south (Baltic Shield) prograded into the area. The onset of progradation is best constrained in the Pechora Sea (Transect 1; Fig. 6) where the lowermost clinoforms have been penetrated by wells and dated to late(st) Permian (Johansen et al., 1993). The wide and deep East Barents Basin experienced additional subsidence which may have been caused by phase changes in the lower crust and/or upper mantle (Gac et al., 2012, 2013). Their preferred model includes Late Devonian-early Carboniferous extension/thinning and associated magmatism giving rise to a thick magmatic underplate and/or widespread intrusions into the lower crust. Subsequently, in the late Permian, compressional deformation may have caused buckling of the lithosphere. Thickening exposed the mafic layer to increased temperatures/pressures which may have triggered phase transitions and a densification of the layer. This may have contributed significantly to the observed rapid subsidence that was not fault-related. In a petroleum exploration context such a model implies a colder basin scenario than if basin subsidence was driven by rifting/regional extension (Gac et al., 2014).

The south Kara Sea is underlain by a rift system assumed to have formed in late Permian-Early Triassic times (Transect 4; Fig. 9) as a result of sinistral transtension (Nikishin et al., 2011). Such a model implies extension along the Pai Khoi margin, which is not in accordance with the sinistral transpression documented by Curtis et al. (*this volume*) along a NW-SE trend parallel to the southern margin of the South Kara Sea. In fact Drachev (2016) argued for an Early Jurassic age of this extensional phase from indirect evidence suggesting deformed basement of Triassic age underlyies the South Kara rifts. Part of the much wider

West Siberian Basin was affected by Permo-Triassic Siberian Trap magmatism (Dobretsov et al., 2013; Kamo et al., 2003). Onshore this resulted in regionally high heat flow and uplift and doming of the crust (Rosen et al., 2009), with concomitant erosion providing detritus to the surrounding Triassic basins (Zhang et al., b *this volume*).

Triassic – Early/Middle Jurassic

The major prograding system reached the western Barents Sea in earliest Triassic time gradually filling in a regional deep water basin (Glørstad-Clark et al., 2010). By Late Triassic time the system had reached all the way to Svalbard in the northwest (Riis et al., 2008; Klausen et al., 2014). Western Spitsbergen was located close to NE Greenland and received sediments with a western provenance (Bue & Andresen, 2014). A thick Upper Triassic depocenter, likely sourced from NE Greenland, developed in the southwestern Barents Sea.

The final upthrusting of Novaya Zemlya (and Taimyr) occurred in Late Triassic (-?Early Jurassic) times, manifested by a prominent angular unconformity in front of the uplifted fold-and-thrust belt (Transect 2; Fig. 7). Here, Jurassic strata overlay deformed Middle-Upper Triassic strata which were eroded during the uplift of Novaya Zemlya (Khlebnikov et al., 2011; Artyushkov et al., 2014; Nikishin et al., 2014, Shipilov, 2015). Two depocenters, separated by a saddle, developed in the eastern Barents Sea (Suslova, 2013, 2014). Westwards, in particular towards Svalbard, the Lower-Middle Jurassic succession thins and locally becomes condensed due to uplift. The compressional regime may have caused uplift of local structural highs. On the eastern side of Novaya Zemlya, in the South Kara Sea, inversion of rift structures has been reported (Nikishin et al., 2011).

Late Jurassic – Early Cretaceous

The Late Jurassic-earliest Cretaceous regional extension in the SW Barents Sea was accompanied by oblique (strike-slip) adjustments along old structural lineaments. This deformation created the Bjørnøya, Tromsø and Harstad basins as prominent rift basins (Transects 1 & 6; Figs. 6 & 11). The evolution of these basins was closely linked to important tectonic phases/events in the North Atlantic-Arctic region (Faleide et al., 1993a). Rifting continued in Early Cretaceous time. A phase of Aptian faulting is documented in the SW Barents Sea, which was part of a deep North Atlantic rift system stretching from the Rockall

Trough to the Bjørnøya Basin. The crust was significantly thinned and nearly reached breakup. As a result a series of very deep Cretaceous basins formed along the rift axis.

Regional uplift associated with the Early Cretaceous High Arctic Large Igneous Province (HALIP) gave rise to a major depositional system characterized by north to south progradation covering most of the Barents Sea (Midtkandal & Nystuen, 2009). Volcanic extrusives are preserved in the northern Barents Sea, mainly on Franz Josef Land and eastern Svalbard, while intrusives are found widespread, particularly in the deep East Barents Basin (Grogan et al., 2000; Minakov et al., 2012b; Polteau et al., 2016; Minakov et al., *this volume*). The magmatism has recently been well dated based on samples from both Svalbard and Franz Josef Land to 122-124 Ma (Corfu et al., 2013).

<u>Late Cretaceous – Paleocene</u>

A mega-shear system linking the NE Atlantic and Arctic regions along the western Barents Sea-Svalbard margin (De Geer Zone) was established in Late Cretaceous-Paleocene times (Faleide et al., 2008). Narrow pull-apart basins formed within this dominantly shear regime-controlled system, which also covered the Wandel Sea Basin in NE Greenland (Håkansson & Pedersen, 2001, 2015). Little or no Upper Cretaceous sediments are preserved in the Barents Sea except in the SW Barents Sea which continued to subside in response to faulting in a pull-apart setting. The prominent Upper Cretaceous hiatus, despite an all-time high global sea level, was probably related to regional uplift associated with renewed magmatism in adjacent areas of the Arctic (North Greenland and Ellesmere Island) and formation of the Alpha Ridge (Tegner et al., 2011). The Barents Shelf subsided again in the late Paleocene and a thick succession accumulated in a regional basin of considerable water depth (Nagy et al., 1997; Ryseth et al., 2003).

<u>Eocene – Oligocene</u>

The western Barents Sea-Svalbard margin developed from this megashear zone which linked the Norwegian-Greenland Sea and the Eurasia Basin during the Eocene opening. The first-order crustal structure along the margin and its tectonic development is mainly the result of three controlling factors: (1) the pre-break-up structure, (2) the geometry of the plate boundary at opening and (3) the direction of relative plate motion. The interplay between these factors gave rise to striking differences in the structural development of the different margin segments of a sheared and/or rifted nature (Faleide et al., 2008). A central rifted segment developed at a releasing bend in the margin southwest of Bjørnøya. This was associated with magmatism in the Vestbakken Volcanic Province both during break-up at the Palaeocene-Eocene transition and later in the Oligocene. A restraining bend SW of Svalbard gave rise to the transpressional Spitsbergen Fold and Thrust Belt (Leever et al., 2011). This was initiated already in the late Paleocene (Jones et al. 2016) and was closely linked to the Eurekan fold belt on Ellesmere Island through North Greenland (Piepjohn et al., 2016). Contractional deformation is also observed in the Barents Sea east of Svalbard, showing that stress related to transpression at the plate boundary west of Svalbard was partitioned and transferred over large distances. Domal structures observed in the central and eastern Barents Sea could also be far-field effects of this compressional regime. However the lack of preserved stratigraphy makes it impossible to further constrain such a model.

Since earliest Oligocene time (magnetic chron 13) Greenland moved with North America in a more westerly direction relative to Eurasia. This gave rise to extension, break-up and onset of seafloor spreading also in the northern Greenland Sea west of Svalbard (Transect 3; Fig. 8). A deepwater gateway between the North Atlantic and Arctic was established sometime in the Miocene (Engen et al., 2008). This had large implications for the paleo-oceanography and regional climate.

The northern Barents Sea margin was expected to be a predominantly rifted margin, formed during separation of the Lomonosov Ridge from the Barents Shelf. However, the study of Minakov et al. (2012a) revealed a narrow transition with steep gradients in crustal thickness, an architecture more characteristic of sheared margins (Transect 5; Fig. 10). They therefore proposed a short-lived initial phase of shear during the Paleocene breakup of the Eurasia Basin. This was further supported by thermo-mechanical modelling (Minakov et al., 2013).

<u>Neogene</u>

The entire Barents Shelf experienced Neogene uplift and erosion. Much of this was related to Plio-Pleistocene glaciation but important pre-glacial tectonic uplift affected western and northern areas, with the strongest uplift centered in the northwest across the Bjørnøya to

Svalbard area (Dimakis et al., 1998; Green & Duddy, 2010; Henriksen et al., 2011b). The subcrop pattern below thin Quaternary cover on the shelf is dominated by Mesozoic units (Sigmond, 2002; Harrison et al., 2011). Erosional products from the uplifted Barents Shelf were transported to major depocenters along the western and northern continental margins bounding the oceanic Norwegian-Greenland Sea and Eurasia Basin respectively. These glacial sediments form fans which developed in front of bathymetric troughs created by erosion associated with ice streams (Andreassen & Winsborrow, 2009; Laberg et al., 2012).

The area in the NW Barents Sea (including Svalbard) which experienced the largest uplift and erosion is characterized by high heat flow, young magmatism (up to recent), and a thin lithosphere (Transects 2 & 3; Figs. 7 & 8; Klitzke et al., 2016). This may reflect mantle processes underneath the NW corner of Eurasia since Miocene separation from Greenland (Vågnes & Amundsen, 1993; Engen et al., 2008). However, the onset of uplift is difficult to constrain.

Summary and conclusions

In this paper we have addressed the lithosphere structure and evolution of the Barents-Kara Sea region. Regional transects at both crustal and lithospheric scales have been used to link deep and shallow structures and processes, as well as to link offshore and onshore areas. These transects (Figs. 6-11), together with the maps from the 3D model (Figs. 2-5), formed the basis for the description and discussion addressing the regional geological evolution with focus on orogenesis and basin development. The main geological events are summarized below.

The study area has been affected by numerous orogenic events forming the crystalline basement of the various geological provinces:

- Precambrian-Cambrian Timanian orogeny is best known onshore Russia in the Timan-Pechora region. Timanian basement extends offshore into the eastern Barents Sea but is difficult to identify in the seismic data beneath deep basin fill intruded by sills. The north Kara Sea is also likely underlain by Timanian basement.

- Silurian-Devonian Caledonian orogeny is well constrained onshore northern Norway. The Caledonian structures continue into the southern Barents Sea where they change orientation from NNE to NNW (towards Svalbard in the north). The geometry of the Caledonian deformation front can be traced using high-resolution magnetic data in the SW Barents Sea. The eastward extension of the Caledonian deformation front in the northern Barents Sea is less certain, but the transition from Caledonian to Timanian basement is expected to be located somewhere between Svalbard and Franz Josef Land.
- Latest Devonian-earliest Carboniferous (Ellesmerian/Svalbardian) deformation affecting western Svalbard is linked to Ellesmere Island in the Canadian Arctic. A considerable strike-slip component gave rise to transpression.
- Carboniferous-Permian Uralian orogeny resulted from the final closure of the Uralian ocean. The Polar Urals on mainland Russia are a prominent and distinct feature but their northward continuation is less certain. Many authors have suggested a continuation to Novaya Zemlya through Pai Khoi, but the deformation there is younger (see below). Taimyr was also affected by the main Uralian event.
- The final upthrusting of Novaya Zemlya occurred in Late Triassic (-?Early Jurassic) time and was associated with sinistral transpression in Pai Khoi.
- Paleogene folding and thrusting affected Ellesmere Island, North Greenland and western Svalbard during the Eurekan/Spitsbergen event. It was initiated in the latest Paleocene by northward movement of Greenland. The main phase occurred during Eocene transpression within the regional shear zone linking seafloor spreading in the NE Atlantic and the Arctic Eurasia Basin.

Regional magmatic events affecting parts of the study area include:

- Widespread Late Devonian (-?early Carboniferous) magmatism. Across the Timan-Varanger region Devonian magamtism is related to rifting.
- Widespread Siberian Trap magmatism. This large igneous province developed at the Permian-Triassic transition. It likely generated a large thermal anomaly, buoyant lithosphere, and regional uplift of the crust. Subsequent erosion of the uplifted dome (resulting from impact of the plume head) would have shed detritus across a wide region, as documented by Arctic sediment provenance investigations.

- The Early Cretaceous High-Arctic large igneous province (HALIP), which is inferred to have formed during opening of the Amerasia Basin. It was centered north of the Canadian Arctic islands, but associated extrusives and intrusives (dykes, sills) are found across the Arctic. This magmatic event would have caused regional uplift of the proto-Arctic region, forming a source area for sedimentary systems prograding southwards on the Barents Shelf and in the Sverdrup Basin.
- Late Cretaceous alkaline magmatism. This mainly affected North Greenland and Ellesmere Island, and likely parts of the conjoined Alpha Ridge.
- Breakup in the NE Atlantic. This occurred around the Paleocene-Eocene transition and was associated with widespread sub-aerial volcanism. Large volumes of extrusive and intrusive rocks are found at the conjugate margins off Norway and east Greenland. This volcanism also affected the central segment of the western Barents Sea margin within the Vestbakken Volcanic Province.

Sedimentary basin development started at different times throughout the study area, as determined by the age of the underlying crystalline basement, and includes the following:

- Early Paleozoic basins. These developed on Timanian basement extending from the Pechora Basin through the eastern Barents Sea to the northern Kara Sea. In the northern Kara Sea the lower Paleozoic succession comprises salt of Ordovician age.
- Late Paleozoic basins. The western Barents Sea was affected by three Late Paleozoic tectonic phases (Late Devonian, Carboniferous and late Permian). The eastern Barents Sea experienced Late Devonian-earliest Carboniferous rifting and magmatism followed by a phase of latest Permian-earliest Triassic rapid regional subsidence. During late Carboniferous and early Permian times a regional carbonate platform covered the entire Barents Shelf.
- Triassic basins. A Triassic regional depositional system, mainly sourced from the uplifted Urals, prograded across the entire Barents Shelf. Lower-Middle Jurassic depocenters developed in a foreland basin to the uplifted Novaya Zemlya fold-and-thrust belt.
- Late Jurassic-Early Cretaceous basins. Deep sedimentary basins developed in the SW Barents Sea in response to major Late Jurassic-Early Cretaceous rifting related to the North Atlantic rift system.

- Late Cretaceous – Paleocene basins. In the SW Barents Sea and NE Greenland Late Cretaceous-Paleocene basins developed within a regional shear zone linking North Atlantic and Arctic rifting.
- Eocene basins. Continental breakup in the earliest Eocene was followed by the evolution of the western Barents Sea-Svalbard and northern Barents Sea margins. Both margins are characterized by a narrow/sharp continent-ocean transition indicating that shear played an important role in the continental breakup and initial opening of the oceanic basins.
- Neogene basins. The entire Barents-Kara shelf was uplifted and eroded during the Neogene. Most of the erosion occurred during the Quaternary northern hemisphere glaciations, but parts of the area were also uplifted and eroded in response to tectonic processes prior to glaciation.

Ackowledgements

This work has been carried out within the CALE (Circum-Arctic Lithosphere Evolution) project funded by IASC, ILP, ExxonMobil, British Petroleum, Statoil, Chevron and Shell. JIF also acknowledges financial support from The Centre for Earth Evolution and Dynamics (CEED) funded by the Research Council of Norway through their Centre of Excellence grant 223272, and from the Research Centre for Arctic Petroleum Exploration (ARCEx), which is funded by the Research Council of Norway (grant number 228107) together with ten academic and nine industry partners. VP acknowledges financial support from the Swedish Research Council. Many thanks also go to the reviewers, S. Drachev and A. Nikishin, who on short notice came back with comprehensive and constructive reviews.

References

Aarseth I., Mjelde, R., Breivik, A.J., Minakov, A., Faleide, J.I., Flueh, E. & Ritske S. Huismans, R.S. 2017. Crustal structure and evolution of the Arctic Caledonides: Results from controlled-source seismology. *Tectonophysics,* **xxx**, xxx–xxx (available online 22 April 2017)

Afanasenkov, A.P., Nikishin, A.M., Unger, A.V., Bordunov, S.I., Lugovaya, O.V., Chikishev, A.A., Yakovishina, E.V. 2016. The tectonics and stages of the geological history of the Yenisei–Khatanga Basin and the conjugate Taimyr Orogen. *Geotectonics,* **50(2)**, 161-178.

Andreassen, K. and Winsborrow, M. 2009. Signature of ice streaming in Bjørnøyrenna, Polar North Atlantic, through the Pleistocene and implications for ice-stream dynamics. *Annals of Glaciology, **50***(**52)**, 17-26.

Anell, I.M., Faleide, J.I. & Braathen, A. 2016. Regional tectono-sedimentary development of the highs and basins of the northwestern Barents Shelf. *Norsk Geologisk Tidsskrift,* **96**, 27-41.

Artyushkov, E.V., Belyaev, I.V., Kazanin, G.S., Pavlov, S.P., Chekhovich, P.A. & Shkarubo, S.I. 2014. Formation mechanisms of ultradeep sedimentary basins: the North Barents basin. Petroleum potential implications. *Russian Geology and Geophysics*, **55**, 649–667.

Barrère, C., Ebbing, J., & Gernigon, L. 2009. Offshore prolongation of Caledonian structures and basement characterisation in the western Barents Sea from geophysical modelling. *Tectonophysics,* **470(1)**, 71-88.

Barrère, C., Ebbing, J., & Gernigon, L. 2011. 3-D density and magnetic crustal characterization of the southwestern Barents Shelf: implications for the offshore prolongation of the Norwegian Caledonides. *Geophysical Journal International*, **184(3)**, 1147-1166.

Bea, F., Fershtater, G. B. & Montero, P. 2002. Granitoids of the Uralides: implications for the evolution of the Orogen. *In*: Brown, D., Juhlin, C. & Puchkov, V. (eds) Mountain Building in the Uralides: Pangea to Present. American Geophysical Union, Washington, DC, Geophysical Monographs, **132**, 211–233.

Bergh, S.G., Braathen, A., Andresen, A. 1997. Interaction of basement-involved and thin-skinned tectonism in the Tertiary fold-thrust belt of central Spitsbergen, Svalbard. *AAPG Bulletin,* **81(4)**, 637-661.

Berglar, K., Franke, D., Lutz, R., Schreckenberger, B. & Damm, V. 2016. Initial Opening of the Eurasian Basin, Arctic Ocean. *Front. Earth Sci.*, **4:91**. doi: 10.3389/feart.2016.00091

Blaich, O.A., Faleide, J.I., Rieder, M., Ersdal, G. & Thyberg, B.I. 2012. Seismic velocities guiding geological interpretation in frontier areas: The Stappen High area, S.W. Barents Sea. *First Break*, **30**, 73-77.

Blaich, O.A., Tsikalas, F. & Faleide, J.I. 2017. New insights into the tectono-stratigraphic evolution of the southern Stappen High and its transition to Bjørnøya Basin, SW Barents Sea. *Marine and Petroleum Geology*, **85**, 89-105.

Blinova, M., Faleide, J.I., Gabrielsen, R.H. & Mjelde, R. 2013. Analysis of structural trends of sub-seafloor stratain the Isfjorden area of the West Spitsbergen Fold-and-Thrust Belt based on multichannel seismic data. *Journal of the Geological Society*, **170 (4)**, 657-668.

Bogatsky, V.I., Bogdanov, N.A., Kostyuchenko, S.I., Senin, B.V., Sobolev, S.F., Shipilov, E.V. & Khain, V.E. 1996. Explanatory notes for the tectonic map of the Barents Sea and the northern part of European Russia, Scale 1:2500000, edited by N.A. Bogdanov and V.E. Khain. Institute of the Lithosphere, Russian Academy of Sciences, Moscow.

Braathen, A., Bergh, S.G., Maher, H.D. 1999. Application of a critical wedge taper model to the Tertiary transpressional fold-thrust belt on Spitsbergen, Svalbard. *Geological Society of America Bulletin*, **111(10)**, 1468-1485.

Breivik, A., Gudlaugsson, S.T. & Faleide, J.I. 1995. Ottar Basin, SW Barents Sea: a major Upper Paleozoic rift basin containing large volumes of deeply buried salt. *Basin Research*, **7**, 299-312.

Breivik, A. J., Mjelde, R., Grogan, P., Shimamura, H., Murai, Y., Nishimura, Y., & Kuwano, A. 2002. A possible Caledonide arm through the Barents Sea imaged by OBS data. *Tectonophysics*, **355(1)**, 67-97.

Breivik, A. J., Mjelde, R., Grogan, P., Shimamura, H., Murai, Y., & Nishimura, Y. 2003. Crustal structure and transform margin development south of Svalbard based on ocean bottom seismometer data. *Tectonophysics*, **369(1)**, 37-70.

Breivik, A. J., Mjelde, R., Grogan, P., Shimamura, H., Murai, Y., & Nishimura, Y. 2005. Caledonide development offshore–onshore Svalbard based on ocean bottom seismometer, conventional seismic, and potential field data. *Tectonophysics*, **401(1**), 79-117.

Bue, E.P. & Andresen, A. 2014. Constraining depositional models in the Barents Sea region using detrital zircon U–Pb data from Mesozoic sediments in Svalbard. Geological Society, London, Special Publications, **386**, 261–279.

Clark, S.A., Faleide, J.I., Hauser, J., Ritzmann, O., Mjelde, R., Ebbing, J., Thybo, H. & Flüh, E. 2013. Stochastic velocity inversion of seismic reflection/refraction traveltime data for rift structure of the southwest Barents Sea. *Tectonophysics*, **593**, 135–150.

Clark, S.A., Glørstad-Clark, E., Faleide, J.I., Schmid, D., Hartz, E.H. & Fjeldskaar, W. 2014. Southwest Barents Sea rift basin evolution: comparing results from backstripping and time-forward modelling. *Basin Research*, **26 (4)**, 550-566.

Corfu, F., Polteau, S., Planke, S., Faleide, J.I., Svensen, H., Zayoncheck, A. & Stolbov, N., 2013. U-Pb geochronology of Cretaceous magmatism on Svalbard and Franz Josef Land, Barents Sea Large Igneous Province. *Geological Magazine*, **150 (6)**, 1127-1135.

Curtis, M.L., Lopez-Mir, B., Scott, R.A. & Howard, J.P., *this volume*. Triassic sinistral transpression along the Pai-Khoi fold-and-thrust belt, Russia: Implications for the structural interpretation of southernmost Novaya Zemlya. *In* Pease, V. and Coakley, B. (eds) Circum Arctic Lithosphere Evolution, Geological Society of London Special Publication 460, xx-xx

Czuba, W., Grad, M., Guterch, A., Majdański, M., Malinowski, M., Mjelde, R., Moskalik, M., Środa, P., Wilde-Piórko, M. & Nishimura, Y. 2008. Seismic crustal structure along the deep transect Horsted'05, Svalbard. *Polish Polar Research*, **29(3)**, 279-290.

Dallmann, W.K. 2015 (Ed.). Geoscience Atlas of Svalbard. Norwegian Polar Institute, Report 148, Tromsø, 292p

Dibner, V.D. (ed) 1998. Geology of Franz Josef Land. Norsk Polarinstituttt, Meddelelser nr. 146, Oslo, pp. 190.

Dick, H. J., Lin, J. & Schouten, H. 2003. An ultraslow-spreading class of ocean ridge. Nature **426**(6965), 405-412.

Dimakis, P., Braathen, B.I., Faleide, J.I., Elverhøi, A. & Gudlaugsson, S.T., 1998. The Cenozoic uplift and erosion of the Svalbard-Barents Sea region. *Tectonophysics*, **300**, 311-327

Dobretsov, N., Vernikovsky, V., Karyakin, Y.V., Korago, E. & Simonov, V. 2013.Mesozoic–Cenozoic volcanism and geodynamic events in the Central and Eastern Arctic. *Russian Geology and Geophysics*, **54**, 874-887.

Drachev, S.S., 2016. Fold belts and sedimentary basins of the Eurasian Arctic. *Arktos*, **2**.

Drachev, S.S., Malyshev, N. & Nikishin, A. 2010. Tectonic history and petroleum geology of the Russian Arctic Shelves: an overview. Geological Society, London, Petroleum Geology Conference series, **7**, 591-619.

Engen, Ø., Faleide, J.I. & Dyreng, T.K. 2008. Opening of the Fram Strait gateway: A review of plate tectonic constraints. *Tectonophysics*, **450**, 51-69.

Engen, Ø., Gjengedal, J.A., Faleide, J.I., Kristoffersen, Y. & Eldholm, O. 2009. Seismic stratigraphy and sediment thickness of the Nansen Basin, Arctic Ocean. *Geophysical Journal International*, **176(3)**, 805-821.

Faleide, J.I., Bjørlykke, K. & Gabrielsen, R. H. 2015. Geology of the Norwegian continental shelf. In: *Petroleum Geoscience: From Sedimentary Environments to rock Physics*. Springer Berlin Heidelberg, 603-637.

Faleide, J.I., Tsikalas, F., Breivik, A.J, Mjelde, R., Ritzmann, O., Engen, Ø., Wilson, J. & Eldholm, O. 2008. Structure and evolution of the continental margin off Norway and the Barents Sea. *Episodes*, **31**, 82-91.

Faleide, J.I., Solheim, A., Fiedler, A., Hjelstuen, B.O., Andersen, E.S. & Vanneste, K. 1996. Late Cenozoic evolution of the western Barents Sea-Svalbard continental margin. *Global and Planetary Change*, **12**, 53-74.

Faleide, J.I., Vågnes, E. & Gudlaugsson, S.T. 1993a. Late Mesozoic-Cenozoic evolution of the southwestern Barents Sea in a regional rift-shear tectonic setting. *Marine and Petroleum Geology*, **10**, 186-214.

Faleide, J.I., Vågnes, E. & Gudlaugsson, S.T. 1993b. Late Mesozoic-Cenozoic evolution of the southwestern Barents Sea. In: Parker, J.R. (ed.) Petroleum geology of Northwest Europe: Proceedings of the 4th Conference. Geological Society, London, 933-950.

Faleide, J.I., Gudlaugsson, S.T. & Jacquart, G. 1984. Evolution of the western Barents Sea. *Marine and Petroleum Geology*, **1**, 123-150.

Gac, S., Klitzke, P., Minakov, A., Faleide, J.I. & Scheck-Wenderoth, M. 2016. Lithospheric strength and elastic thickness of the Barents Sea and Kara Sea region. *Tectonophysics*, **691**, 120-132.

Gac, S., Huismans, R.S., Simon, N.S.C., Faleide, J.I. & Podladchikov, Yu.Yu. 2014. Effects of lithosphere buckling on subsidence and hydrocarbon maturation: A case study from the ultra-deep East Barents Sea basin. *Earth and Planetary Science Letters*, **407**, 123-133.

Gac, S., Huismans, R.H., Simon, N.S.C., Podladchikov, Yu.Yu. & Faleide, J.I. 2013. Formation of intracratonic basins by lithospheric shortening and phase changes: a case study from the ultra-deep East Barents Sea basin. *Terra Nova*, **25 (6)**, 459-464.

Gac, S., Huismans, R., Podladchikov, Y. & Faleide, J.I. 2012. On the origin of the ultra deep East Barents Sea basin. *Journal of Geophysical Research*, **117**, B04401.

Gaina, C., Gernigon, L. & Ball, P. 2009. Palaeocene-Recent plate boundaries in the NE Atlantic and the formation of the Jan Mayen microcontinent. *Journal of the Geological Society*, **166**, 601-616.

Gaina, C., Werner, S.C., Saltus, R. & Maus, S. 2011. Circum-Arctic mapping project: new magnetic and gravity anomaly maps of the Arctic. Geol. Soc. London, Mem. 35, 39–48. doi:10.1144/M35.3

Gee, D.G., Bogolepova, O.K. & Lorenz, H. 2006. The Timanide, Caledonide and Uralide orogens in the Eurasian high Arctic, and relationships to the palaeo-continents Laurentia, Baltica and Siberia. Geological Society, London, Mem. 32, 507-520.

Geissler, W.H. & Jokat, W. 2004. A geophysical study of the northern Svalbard continental margin. *Geophysical Journal International*, ***158*** **(1)**, 50-66.

Geissler, W.H., Jokat, W. & Brekke, H. 2011. The Yermak Plateau in the Arctic Ocean in the light of reflection seismic data-implication for its tectonic and sedimentary evolution. *Geophysical Journal International*, **187(3)**, 1334-1362.

Gernigon, L. & Brönner, M. 2012. Late Palaeozoic architecture and evolution of the southwestern Barents Sea: insights from a new generation of aeromagnetic data. *Journal of the Geological Society*, **169(4**), 449-459.

Gernigon, L., Brönner, M., Roberts, D., Olesen, O., Nasuti, A. & Yamasaki, T. 2014. Crustal and basin evolution of the southwestern Barents Sea: from Caledonian orogeny to continental breakup. *Tectonics*, **33(4)**, 347-373.

Glørstad-Clark, E., Faleide, J.I., Lundschien, B.A. & Nystuen, J.P. 2010. Triassic seismic sequence stratigraphy and paleogeography of the western Barents Sea area. *Marine and Petroleum Geology*, **27**, 1448-1475.

Grad, M., Mjelde, R., Krysinski, L., Czuba, W., Libak, A., Guterch, A. & IPY Project Group 2015. Geophysical investigations of the area between the Mid-Atlantic Ridge and the Barents Sea: From water to the lithosphere-asthenosphere system. *Polar Science*, **9**, 168-183.

Green, P.F., & Duddy, I.R. 2010. Synchronous exhumation events around the Arctic including examples from Barents Sea and Alaska North Slope. *In: Vining, B.A. & Pickering, S. C. (Eds.) Petroleum Geology: From Mature Basins to New Frontiers - Proceedings of the 7th Petroleum Geology Conference. Petroleum Geology Conference Series, Geological Society, London*, ***7***, 633–644.

Grogan, P., Nyberg, K., Fotland, B., Myklebust, R., Dahlgren, S. & Riis, F. 2000. Cretaceous magmatism south and east of Svalbard: evidence from seismic reflection and magnetic data. *Polarforschung*, ***68***, 25-34.

Gudlaugsson, S.T., Faleide, J.I., Johansen, S.E. & Breivik, A. 1998. Late Palaeozoic structural development of the south-western Barents Sea. *Marine and Petroleum Geology*, **15**, 73-102.

Gudlaugsson, S.T. & Faleide, J.I. 1994. The continental margin between Spitsbergen and Bjørnøya. *Norsk Polarinst. Meddel.*, **130**, 11-13.

Gudlaugsson, S.T., Faleide, J.I., Fanavoll, S. & Johansen, B. 1987. Deep seismic reflection profiles across the western Barents Sea. *Geophysical Journal of the Royal Astronomical Society*, **89**, 273-278.

Guise, P.G. & Roberts, D. 2002. Devonian ages from 40Ar/39Ar dating of plagioclase in dolerite dikes, eastern Varanger Peninsula, North Norway. *Norges geologiske undersøkelse Bulletin*, **440**, 27–37.

Harrison, J.C., St-Onge, M.R., Petrov, O.V., Strelnikov, S.I., Lopatin, B.G., Wilson, F.H., Tella, S., Paul, D., Lynds, T., Shokalsky, S.P., Hults, C.K., Bergman, S., Jepsen, H.F. & Solli, A. 2011. Geological map of the Arctic / Carte géologique de l'Arctique; Geological Survey of Canada, Map 2159A, scale 1:5 000 000.

Hauser, J., Dyer, K., Pasyanos, M., Bungum, H., Faleide, J.I., Clark, S.A. & Schweitzer, J. 2011. A Probabilistic Seismic Model for the European Arctic. *Journal of Geophysical Research*, **116**, B01303.

Henriksen, E., Ryseth, A.E., Larssen, G.B., Heide, T., Rønning, K., Sollid, K. & Stoupakova, A.V. 2011a. Tectonostratigraphy of the greater Barents Sea: implications for petroleum systems. Geological Society, London, Memoirs **35**, 163-195.

Henriksen, E., Bjørnseth, H.M., Hals, T.K., Heide, T., Kiryukhina, T., Kløvjan, O.S., Larssen, G.B., Ryseth, A.E., Rønning, K., Sollid, K. & Stoupakova, A. 2011b. Uplift and erosion of the greater Barents Sea: impact on prospectivity and petroleum systems. Geological Society, London, Memoirs **35**, 271-281.

Hjelstuen, B.O., Elverhøi, A. & Faleide, J.I. 1996. Cenozoic erosion and sediment yield in the drainage area of the Storfjorden Fan. *Global and Planetary Change*, **12(1-4)**, 95-117.

Håkansson, E. & Pedersen, S.A.S. 2001. The Wandel Hav strike-slip mobile belt—a Mesozoic plate boundary in North Greenland. *Bulletin of the Geological Society of Denmark*, **48**, 149-158.

Håkansson, E. & Pedersen, S.A.S. 2015. A healed strike-slip plate boundary in North Greenland indicated through associated pull-apart basins. Geological Society, London, Special Publications **413**, 143-169.

Indrevær, K., Bergh, S.G., Koehl, J.B., Hansen, J.A., Schermer, E.R. & Ingebrigtsen, A. 2013. Post-Caledonian brittle fault zones on the hyperextended SW Barents Sea margin: New insights into onshore and offshore margin architecture. *Norwegian Journal of Geology*, **93(3-4)**, 167-188.

Indrevær, K., Stunitz, H., & Bergh, S.G. 2014. On Palaeozoic–Mesozoic brittle normal faults along the SW Barents Sea margin: fault processes and implications for basement permeability and margin evolution. *Journal of the Geological Society*, **171(6)**, 831-846.

Inger, S., Scott, R.A. & Golionko, B.G. 1999. Tectonic evolution of the Taimyr Peninsula, northern Russia: implications for Arctic continental assembly. *Journal of the Geological Society*, **156**, 1069-1072.

Ivanova, N.M., Sakulina, T.S., Belyaev, I.V., Matveev, Y.I., & Roslov, Y.V. 2011. Depth model of the Barents and Kara seas according to geophysical surveys results. Geological Society, London, Memoirs **35**, 209-221.

Jackson, H.R., Sweeney, J.F. et al. 1993. International Lithosphere Program: Global Geoscience Transect #10, Arctic Ocean: Alaska-Norway. Atlantic Geoscience Centre, Geol. Surv. Canada.

Jakobsson, M., Mayer, L., Coakley, B., Dowdeswell, J.A., Forbes, S., Fridman, B., Hodnesdal, H., Noormets, R., Pedersen, R., Rebesco, M., Schenke, H.W., Zarayskaya, Y., Accettella, D., Armstrong, A., Anderson, R.M., Bienhoff, P., Camerlenghi, A., Church, I., Edwards, M., Gardner, J. V., Hall, J.K., Hell, B., Hestvik, O., Kristoffersen, Y., Marcussen, C., Mohammad, R., Mosher, D., Nghiem, S. V., Pedrosa, M.T., Travaglini, P.G., & Weatherall, P. 2012. The International Bathymetric Chart of the Arctic Ocean (IBCAO) Version 3.0. Geophysical Research Letters 39, 1–6. doi:10.1029/2012GL052219

Johansen, S.E., B.K. Ostisty, Ø. Birkeland, Y.F. Fedorovsky, V.N. Martirosjan, O. Bruun Christensen, S.I. Cheredeev, E.A. Ignatenko & L. S. Margulis 1993. Hydrocarbon potential in the Barents Sea region: Play distribution and potential, in Artic Geology and Petroleum Potential, NPF Spec. Publ., vol. 2, edited by T.O. Vorren et al., 273–320, Elsevier, Amsterdam.

Johansson, Å., Gee, D.G., Larionov, A.N., Ohta, Y. & Tebenkov, A.M. 2005. Grenvillian and Caledonian evolution of eastern Svalbard–a tale of two orogenies. *Terra Nova*, **17(4)**, 317-325.

Jokat, W., Weigelt, E., Kristoffersen, Y., Rasmussen, T. & Schöone, T. 1995. New insights into the evolution of the Lomonosov Ridge and the Eurasian Basin. *Geophysical Journal International*, **122(2)**, 378-392.

Jokat, W. & Micksch, U. 2004. Sedimentary structure of the Nansen and Amundsen basins, Arctic Ocean. *Geophysical Research Letters,* **31 (2)**, L02603.

Jokat, W., Lehmann, P., Damaske, D. & Bradley Nelson, J. 2016. Magnetic signature of North-East Greenland, the Morris Jesup Rise, the Yermak Plateau, the central Fram Strait: Constraints for the rift/drift history between Greenland and Svalbard since the Eocene. *Tectonophysics*, **691**, 98-109.

Jones, M.T., Trygvason, E.G., Shephard, G., Svensen, H., Jochmann, M., Friis, B., Augland, L. E.; Jerram, D.A. & Planke, S. 2016. Provenance of bentonite layers in the Palaeocene strata of the Central Basin, Svalbard: implications for magmatism and rifting events around the onset of the North Atlantic Igneous Province. *Journal of Volcanology and Geothermal Research*, **327**, 571-584.

Kamo, S.L., Czamanske, G.K., Amelin, Y., Fedorenko, V.A., Davis, D. & Trofimov, V. 2003. Rapid eruption of Siberian flood-volcanic rocks and evidence for coincidence with the Permian–Triassic boundary and mass extinction at 251 Ma. *Earth and Planetary Science Letters*, **214**, 75-91.

Klausen, T.G., Ryseth, A.E., Helland-Hansen, W., Gawthorpe, R. & Laursen, I. 2014. Spatial and temporal changes in geometries of fluvial channel bodies from the Triassic Snadd Formation of offshore Norway. *Journal of Sedimentary Research*, **84**, 567–585.

Klitzke, P., Sippel, J., Faleide, J.I. & Scheck-Wenderoth, M. 2016. A 3D Gravity and Thermal Model for the Barents Sea and Kara Sea. *Tectonophysics*, **691**, 120-132.

Klitzke, P., Faleide, J.I., Scheck-Wenderoth, M., Sippel, J. 2015. A lithosphere-scale structural model of the Barents Sea and Kara Sea region. *Solid Earth*, **6**, 153-172.

Khlebnikov, P.A., Belenky, V.Ya., Peshkova, I.N., Kazanin, G.S., Shkarubo, S.I., Pavlov, S.P. & Shlykova, V.V. 2011. Geological structure and petroleum potential of the eastern flank of the Northern Barents Basin. *Geological Society, London, Memoirs* 35, 261-269.

Khutorskoi, M.D., Viskunova, K.G., Podgornykh, L.V., Suprunenko, O.I., & Akhmedzyanov, V.R. 2008. A temperature model of the crust beneath the Barents Sea: investigations along geotraverses, *Geotectonics*, **42**, 125-136.

Knudsen, C., Hopper, J.R., Bierman, P.R., Bjerager, M., Funck, T., Green, P.F., Ineson, J.R., Japsen, P., Marcussen, C., Sherlock, S.C. & Thomsen, T.B., *this volume*. Samples from the Lomonosov Ridge place new constraints on the geological evolution of the Arctic Ocean. *In* Pease, V. and Coakley, B. (eds) Circum Arctic Lithosphere Evolution, Geological Society of London Special Publication 460, xx-xx

Krysiński, L., Grad, M., Mjelde, R., Czuba, W. & Guterch, A. 2013. Seismic and density structure of the lithosphere− asthenosphere system along transect Knipovich Ridge− Spitsbergen− Barents Sea–geological and petrophysical implications. *Polish Polar Research*, **34(2)**, 111-138.

Laberg, J.S., Andreassen, K. & Vorren, T.O. 2012. Late Cenozoic erosion of the high-latitude southwestern Barents Sea shelf revisited. *Geological Society of America Bulletin*, **124(1-2**), 77-88.

Lacombe, O. & Bellahsen, N. 2016. Thick-skinned tectonics and basement-involved fold–thrust belts: insights from selected Cenozoic orogens. *Geological Magazine*, **153** (5-6), 763–810.

Larionov, A.N., Andreichev, V.A. & Gee, D. 2004. The Vendian alkaline igneous suite of northern Timan: ion microprobe U-Pb zircon ages of gabbros and syenite. Geological Society, London, Memoirs, **30**, 69-74.

Larssen, G.B., Elvebakk, G., Henriksen, L.B., Kristensen, S.-E., Nilsson, I., Samuelsberg, T.J., Svånå, T.A., Stemmerik, L. & Worsley, D. 2005. Upper Palaeozoic lithostratigraphy of the southern part of the Norwegian Barents Sea. *Norges geologiske undersøkelse Bulletin*, **444**, 3-45.

Leever, K.A., Gabrielsen, R.H., Faleide, J.I. & Braathen, A. 2011. A transpressional origin for the West Spitsbergen fold-and-thrust belt: Insight from analog modeling. *Tectonics*, **30**, TC2014.

Levshin, A.L., Schweitzer, J., Weidle, C., Shapiro, N.M. & Ritzwoller, M.H. 2007. Surface wave tomography of the Barents Sea and surrounding regions. *Geophysical Journal International*, **170(1)**, 441-459.

Ljones, F., Kuwano, A., Mjelde, R., Breivik, A., Shimamura, H., Murai, Y. & Nishimura, Y. 2004. Crustal transect from the North Atlantic Knipovich Ridge to the Svalbard Margin west of Hornsund. *Tectonophysics*, **378**, 17-41.

Lorenz, H., Pystin, A.,, Olovyanishnikov, V. & Gee, D. 2004. Neoproterozoic high-grade metamorphism of the Kanin Peninsula, Timanide Orogen, northern Russia. In: Gee & Pease (eds) The Neoproterozoic Timanide Orogen of Eastern Baltica. Geological Society, London, Memoir **30**, 59-68.

Lorenz, H., Gee, D.G. & Whitehouse, M.J. 2007. New geochronological data on Palaeozoic igneous activity and deformation in the Severnaya Zemlya Archipelago, Russia, and implications for the development of the Eurasian Arctic margin. *Geological Magazine*, **144** (1), 105-125.

Lorenz, H., Maennik, P., Gee, D.G. et al., 2008. Geology of the Severnaya Zemlya Archipelago and the North Kara Terrane in the Russian high Arctic. *International Journal of Earth Sciences*, **97** (3), 519-547.

Luosto, U., Flueh. E., Lund, C.-E. and Working Group 1989. The crustal structure along the Polar Profile from seismic refraction. In: R. Freeman, M. von Knorring, H. Korhonen. C. Lund and St. Mueller (Editors), The European Geo- traverse, Part 5: The Polar Profile. *Tectonophysics*, **162**, 51-85.

Malyshev, N.A., Nikishin, V.A., Nikishin, A.M., Obmetko, V.V., Martirosyan, V.N., Kleshchina, L.N. & Reydik, Yu.V. 2012a. A new model of the geological structure and evolution of the North Kara Sedimentary Basin. *Dokladdy Earth Science*, **445** (1), 791-795.

Malyshev, N. A., Nikishin, V. A., Obmetko, V. V., Ikhsanov, B. I., Reydik, Y. V., Sitar, K. A. & Shapabaeva, D. S. 2012b. Geological Structure and Petroleum System of South Kara Basin, in: 5th EAGE St. Petersburg International Conference and Exhibition on Geosciences – Making the Most of the Earths Resources, Saint Petersburg 2012, doi:10.3997/2214-4609.20143593

Marello, L., Ebbing, J. & Gernigon, L. 2010. Magnetic basement study in the Barents Sea from inversion and forward modelling. *Tectonophysics*, **493**, 153-171.

Marello, L., Ebbing, J. & Gernigon, L. 2013. Basement inhomogeneities and crustal setting in the Barents Sea from a combined 3D gravity and magnetic model. *Geophysical Journal International*, **193**, 557-584

Marshall, C., Uguna, J., Large, D.J., Meredith, W., Jochmann, M., Friis, B., Vane, C., Spiro, B.F., Snape, C.E. & Orheim, A. 2015. Geochemistry and petrology of palaeocene coals from Spitzbergen - Part 2: Maturity variations and implications for local and regional burial models. *International Journal of Coal Geology*, **143**, 1–10.

Maslov, A.V. 2004. Riphean and Vendian sedimentary sequences of the Timanides and Uralides, the eastern periphery of the East Euopean Craton. In: Gee & Pease (eds) The Neoproterozoic Timanide Orogen of Eastern Baltica. Geological Society, London, Memoirs **30**, 19-36.

Minakov, A., Yarushina, V, Faleide, J. I., Krupnova, N., Sakoulina, T., Dergunov, N. & Glebovsky, V., *this volume*. Dyke emplacement and crustal structure within a continental large igneous province - northern Barents Sea. *In* Pease, V. and Coakley, B. (eds) Circum Arctic Lithosphere Evolution, Geological Society of London Special Publication XX, xx-xx

Minakov, A., Faleide, J.I., Glebovsky, V.Yu. & Mjelde, R. 2012a. Structure and evolution of the northern Barents–Kara Sea continental margin from integrated analysis of potential fields, bathymetry and sparse seismic data. *Geophysical Journal International*, **188**, 79-102.

Minakov, A., Mjelde, R., Faleide, J.I., Flueh, E.R., Dannowski, A. & Keers, H. 2012b. Mafic intrusions east of Svalbard imaged by active-source seismic tomography. *Tectonophysics*, **518**, 106-118.

Minakov, A.N., Podladchikov, Yu.Yu., Faleide, J.I. & Huismans, R.S. 2013. Rifting assisted by shear heating and formation of the Lomonosov Ridge. *Earth and Planetary Science Letters*, **373**, 31-40.

Midtkandal, I. & Nystuen, J.P. 2009. Depositional architecture of a low-gradient ramp shelf in an epicontinental sea: the lower Cretaceous of Svalbard. *Basin Research*, ***21*** (5), 655-675.

Nagy, J., Kaminski, M.A., Johnsen, K. & Mitlehner, A.G. 1997. Foraminiferal, palynomorph, and diatom biostratigraphy and paleoenvironments of the Torsk Formation: A reference section for the Paleocene-Eocene transition in the western Barents Sea. In: Hass, H.C. & Kaminski, M.A. (eds.) Contributions to the

Micropaleontology and Paleoceanography of the Northern North Atlantic. *Grzybowski Foundation Special Publication,* **5,** 15-38.

Nikishin, A.M., Ziegler, P.A., Stephenson, R.A., Cloetingh, S.A.P.L., Furne, A.V., Fokin, P.A., Ershov, A.V., Bolotov, S.N., Korotaev, M.V., Alekseev, A.S., Gorbachev, V.I., Shippilov, E.V., Lankreijer, A., Bembinova, E.Y. & Shalimov, I.V. 1996. Late Precambrian to Triassic history of the eastern European craton: Dynamics of sedimentary basin evolution. *Tectonophysics*, **268**, 23-63.

Nikishin, V. A., Malyshev, N. A., Nikishin, A. M. & Obmetko, V. V. 2011. The Late Permian-Triassic system of rifts of the South Kara sedimentary basin. *Moscow University Geology Bulletin*, **66**, 377–384.

Nikishin, A.M., Malyshev, N.A. & Petrov, E.I. 2014. Geological structure and history of the Arctic Ocean. EAGE Publications,

Olovyanishnikov, V.G., Siedlecka, A. & Roberts, D. 2000. Tectonics and sedimentation of the Meso- to Neoproterozoic Timan-Varanger Belt along the northeastern margin of Baltica. *Polarforschung*, **68**, 269-276.

Otto, S.C. & Bailey, R.J. 1995. Tectonic evolution of the northern Ural Orogen. *Journal of the Geological Society*, **152**, 903–906.

Pavlis, N.K., Holmes, S.A., Kenyon, S.C. & Factor, J.K. 2012. The Development and Evaluation of the Earth Gravitational Model 2008 (EGM2008). *Journal of Geophysical Research - Solid Earth*, **117**, B04406.

Pease, V., 2011. Eurasian Orogens and Arctic Tectonics: An overvew. In: Spencer, A. M., Embry, A. F., Gautier, D. L., Stoupakova, A. V. & Sørensen, K. (eds) Arctic Petroleum Geology. Geological Society, London, Memoir **35**, 311–324.

Pease, V., 2012. The Buotankaga River traverse. Polarforskningsekretariatet 2012 Årsbok, 22-23.

Pease, V., 2013. The DeLong Islands. Polarforskningsekretariatet 2013, http://polarforskningsportalen.se/arktis/expeditioner/de-long

Pease, V. & Scott, R.A. 2009. Crustal affinities in the Arctic Uralides, northern Russia: significance of detrital zircon ages from Neoproterozoic and Palaeozoic sediments in Novaya Zemlya and Taimyr. *Journal of the Geological Society*, **166**, 517-527.

Pease, V., Gee, D., Lopatin, B., 2001. Is Franz Josef Land affected by Caledonian deformation? European Union of Geosciences Abstracts 5, 757 (abstract).

Pease, V., Drachev, S., Stephenson, R. & Zhang, X. 2014. Arctic lithosphere - A review. *Tectonophysics*, **625**, 1-25.

Pease, V., Kuzmichev, A. & Danukalova, M.K. 2015. Late Paleozoic zircon provenance of the New Siberian Islands and implications for late Cretaceous Arctic reconstructions. *Journal of the Geological Society* (London), **72**, 1-4.

Pease, V., Scarrow, J.H., Nobre Silva, I.G. & Cambeses, A. 2016. Devonian magmatism in the Timan Range, Arctic Russia — subduction, post-orogenic extension, or rifting? *Tectonophysics*, **691**, 185-197.

Petersen, T.G., Thomsen, T.B., Olaussen, S. & Stemmerik, L. 2016. Provenance shifts in an evolving Eurekan foreland basin: the Tertiary Central Basin, Spitsbergen. *Journal of the Geological Society*, **173**, 634–648.

Petrov, G.A., Ronkin, Yu.L., Maslov, A.V., Svyazhina, I.A., Rybalka, A.V. & Lepikhina, O.P. 2008. Timing of the onset of collision in the central and northern Urals. *Doklady Earth Sciences*, **422**, 1050–1055.

Piepjohn, K. & vonGossen, W., this volume. A structural transect through Ellesmere Island – superimposed Paleozoic Ellesmerian and Cenozoic Eurekan deformation. In: Pease & Coakley (eds) Circum-Arctic Lithosphere Evolution, Geological Society, London, Special Publication XX, xx-xx.

Piepjohn, K., vonGossen, W. & Tessensohn, F. 2016. The Eurekan deformation in the Arctic: An outline. *Journal of the Geological Society*, **173**, 1007-1024.

Piepjohn, K., Brinkmann, L., Grewing, A. & Kerp, H. 2000. New data on the age of the uppermost ORS and the lowermost post-ORS strata in Dickson Land (Spitsbergen) and implications for the age of the Svalbardian deformation. *Geological Society, London, Special Publications,* **180**, 603-609.

Polteau, S., Hendriks, B.W.H., Planke, S., Ganerød, M., Corfu, F., Faleide, J.I., Midtkandal, I., Svensen, H. & Myklebust, R. 2016. The Early Cretaceous Barents Sea sill complex: Distribution, 40Ar/39Ar geochronology, and implications for carbon gas formation. *Palaeogeography, Palaeoclimatology, Palaeoecology*, **441**, 83-95.

Prestvik, T. 1978. Cenozoic Plateau Lavas of Spitsbergen: A Geochemical Study. *Norsk Polarinst. Årbok*,

Puchkov, V., Ernst, R.E., Hamilton, M.A., Söderlund, U. & Sergeeva, N. 2016. A Devonian >2000-km-long dolerite dyke swarm-belt and associated basalts along the Urals-Novozemelian fold-belt: Part of an East-European (Baltica) LIP tracing the Tuzo Superswell. *GFF*, **138(1**), 6-16.

Rickers, F., Fichtner, A. & Trampert, J. 2013. The Iceland–Jan Mayen plume system and its impact on mantle dynamics in the North Atlantic region: evidence from full-waveform inversion. *Earth and Planetary Science Letters*, **367**, 39-51.

Riis, F., Lundschien, B., Høy, T., Mørk, A. & Mørk, M.B. 2008. Evolution of the Traissic shelf in the Northern Barents Sea region. *Polar Research*, **27**, 318–338.

Ritzmann, O. & Faleide, J.I. 2007. The Caledonian basement of the western Barents Sea. Tectonics, **26**, TC5014.

Ritzmann, O. & Faleide, J.I. 2009. The crust and mantle lithosphere in the Barents Sea/Kara Sea region. *Tectonophysics*, **470**, 89-104.

Ritzmann, O., Maercklin, N., Faleide, J.I., Bungum, H., Mooney, W. & Detweiler, S. 2007. A 3D geophysical model of the crust in the Barents Sea region: Model construction and basement characterisation. *Geophysical Journal International*, **170**, 417-435.

Roslov, Yu.V., Sakoulina, T.S. & Pavlenkova, N.I. 2009. Deep seismic investigations in the Barents and Kara Seas. *Tectonophysics*, **472**, 301–308.

Rosen, O., Soloviev, A. & Zhuravlev, D. 2009. Thermal evolution of the northeastern Siberian Platform in the light of apatite fission ‐ track dating of the deep drill core. *Izvestiya, Physics of the Solid Earth*, **45**, 914-931.

Ryseth, A., Augustson, J.H., Charnock, M., Haugerud, O., Knutsen, S.M., Midbøe, P.S., Opsal, J.G. & Sundsbø, G. 2003. Cenozoic stratigraphy and evolution of the Sørvestsnaget Basin, southwestern Barents Sea. *Norwegian Journal of Geology*, **83** (2), 107-130.

Sakoulina, T.S., Pavlenkova, G.A. & Kashubin, S.N. 2015. Structure of the Earth's crust in the northern part of the Barents–Kara region along the 4-AR DSS profile. *Russian Geology and Geophysics*, **56**, 1622–1633.

Sakoulina, T.S., Kashubin, S.N. & Pavlenkova, G.A. 2016. Deep Seismic Soundings on the 1_AP Profile in the Barents Sea: Methods and Results. *Izvestiya, Physics of the Solid Earth,* **52 (4)**, 572–589.

Saunders, A.D., Jones, S.M., Morgan, L.A., Pierce, K., Widdowson, M. & Xu, Y.G. 2007. Regional uplift associated with continental large igneous provinces: the roles of mantle plumes and the lithosphere. *Chemical Geology*, **241(3)**, 282-318.

Scarrow, J.H., Hetzel, R., Gorozhanin, V.M., Dinn, M., Glodny, J., Gerdes, A., Ayala, C. & Montero, P. 2002. Four decades of geochronological work in the southern and middle Urals: a review. In: Brown, D., Juhlin, C. & Puchkov, V. (eds) Mountain Building in the Uralides: Pangea to Present. AGU, Washington, DC, Geophysical Monographs **132**, 233–256.

Scott, R., Howard, J., Guo, L., Schekoldin, R. & Pease, V. 2010. Offset and curvature of the Novaya Zemlya fold-and-thrust belt, Arctic Russia. In Vining, B.A. and Pickering, S.C. (eds) Petroleum Geology: From Mature Basins to New Frontiers, Petroleum Conferences, Geological Society of London, 645-657.

Shipilov, E.V. 2015. Late Mesozoic Magmatism and Cenozoic Tectonic Deformations of the Barents Sea Continental Margin: Effect on Hydrocarbon Potential Distribution. *Geotectonics,* **49 (1)**, 53–74.

Sigmond, E.M.O. 2002. Geological map of land and sea areas of North Europe, scale 1:4 million. Geological Survey of Norway.

Sobornov, K. 2013. Structure and Petroleum Habitat of the Pay Khoy-Novaya Zemlya Foreland Fold Belt, Timan Pechora, Russia. AAPG Search and Discovery Article #10554.

Sobornov, K. 2015. Structural relationships and development of the Pay Khoy and Polar Urals fold belts, Russia. 3P-Arctic, The Polar Petroleum Potential, Stavanger, October 2015.

Stoupakova, A.V., Henriksen, E., Burlin, Y.K., Larsen, G.B., Milne, J.K., Kiryukhina, T.A., Golynchik, P.O., Bordunov, S.I., Ogarkova, M.P. & Suslova, A.A. 2011. The geological evolution and hydrocarbon potential of the Barents and Kara shelves. *Geological Society, London, Memoirs 35*, 325-344.

Stoupakova, A.V., Kirykhina, T.A., Suslova, A.A., Kirykhina, N.M., Sautkin, R.S. & Bordunov, S.I. 2012. Structure and Hydrocarbon Prospects of the Russian Western Arctic Shelf. Offshore Technology Conference paper, *Arctic Technology Conference* (Houston, December 2012).

Stoupakova A.V., Bordunov S.I., Sautkin R.S., Suslova A.A., Peretolchin S.A. & Sidorenko S.A. 2013. Russian Arctic oil and gas basins (In Russian). *Oil and Gas Geology*, **3**, 30-47.

Suslova, A.A. 2013. Seismostratigraphic Complex of Jurassic Deposits, Barents Sea Shelf. *Moscow University Geology Bulletin*, **68** (3), 207–209.

Suslova, A.A. 2014. Seismostratigraphic analysis and petroleum potential prospects of Jurassic deposits, Barents Sea Shelf (in Russian). Petroleum geology – theoretical and applied studies (ISSN 2070-5379), **9**(2).

Tegner, C., Storey, M., Holm, P.M., Thorarinsson, S.B., Zhao, X., Lo, C.-H. & Knudsen, M.F. 2011. Magmatism and Eurekan deformation in the High Arctic Large Igneous Province: 40Ar–39Ar age of Kap Washington Group volcanics, North Greenland. *Earth and Planetary Science Letters*, **303**, 203–214.

Tsikalas, F., Faleide, J.I., Eldholm, O. & Blaich, O.A. 2012. The NE Atlantic conjugate Margins. In: Roberts, D.G. & Bally, A.W., Phanerozoic Passive Margins, Cratonic Basins and Global Tectonic Maps, Elsevier, DOI: 10.1016/B978-0-444-56357-6.00004-4.

Vernikovsky, V.A. 1995. Riphean and Paleozoic metamorphic complexes of the Taimyr foldbelt - conditions of formation. *Petrology*, **3** (1), 55-72.

Vogt, P.R., Taylor, P.T., Kovacs, L.C. & Johnson, G.L. 1979. Detailed aeromagnetic investigation of the Arctic Basin. *Journal of Geophysical Research - Solid Earth*, **84**, 1071–1089.

Vogt, P.R., Jung, W.-Y. & Brozena, J. 1998. Arctic margin gravity highs: Deeper meaning for sediment depocenters? *Marine Geophysical Researches*, **20**, 459–477.

Vågnes E. & Amundsen H.E.F. 1993. Late Cenozoic uplift and volcanism on Spitsbergen: caused by mantle convection? *Geology*, **21**, 251–254.

Wilson, M., Wijbrans, J., Fokin, P.A., Nikishin, A.M., Gorbachev, V.I. & Nazarevich, B.P. 1999. 40Ar/39Ar dating, geochemistry and tectonic setting of Early Carboniferous dolerite sills in the Pechora basin, foreland of the Polar Urals. *Tectonophysics*, **313**, 107-118.

Worsley, D., Agdestein, T., Gjelberg, J.G., Kirkemo, K., Mørk, A., Nilsson, I., Olaussen, S., Steel, R.J. & Stemmerik, L. 2001. The geological evolution of Bjørnøya, Arctic Norway: implications for the Barents Shelf. *Norsk Geologisk Tidsskrift*, **81**, 195-234.

Zhang, W., Roberts, D. & Pease, V. 2016. Provenance of sandstonefrom Caledonian nappes in Finnmark, Norway: Implications for Neoproterozoic–Cambrian palaeogeography. *Tectonophysics*, **691**, 198-205.

Zhang, X., Pease, V., Carter, A., Scott, R. *this volume a*. Exhumation history of Novaya Zemlya: New insights from geochronology and thermochronology. *In* Pease, V. and Coakley, B. (eds) Circum Arctic Lithosphere Evolution, Geological Society of London Special Publication 460, xx-xx

Zhang, X., Pease, V., Carter, A., Kostuychenko, S. & Scott, R. *this volume b*. Timing of exhumation and deformation across the Taimyr fold and thrust belt from apatite fission track dating and balanced cross-sections. *In* Pease, V. and Coakley, B. (eds) Circum Arctic Lithosphere Evolution, Geological Society of London Special Publication 460, xx-xx

Zhang, X., Pease, V., Skogseid, J. & Wohlgemuth-Ueberwasser, C. 2016. Reconstruction of tectonic events on the northern Eurasia margin of the Arctic, from U-Pb detrital zircon provenance investigations of late Paleozoic to Mesozoic sandstones in southern Taimyr Peninsula. *Geological Society of America Bulletin*, **128**, 29-46. doi:10.1130/B31241.1.

Zhang, X., Pease, V., Omma, J. & Benedictus, A. 2015. Provenance of Late Carboniferous to Jurassic sandstones for southern Taimyr, Arctic Russia: A comparison of heavy mineral analysis by optical and QEMSCAN methods. *Sedimentary Geology*, **329**, 166-176.

Zhang, X., Omma, J., Pease, V. & Scott, R. 2013. Provenance study of late Paleozoic-Mesozoic sandstones from the Taimyr Peninsula, Arctic Russia. In: Schmidt (ed) Sedimentary Basins and Orogenic Belts, Geosciences 3, 502-527. doi:10.3390/geosciences3030502.

Zonenshain, L.P., Kuzmin, M.I. & Natapov, L.M. 1990. Geology of the USSR: a plate tectonic synthesis. Geodynamic Series, vol. 21. Americam Geophysical Union,Washington DC, p. 242.

Figures

Figure 1

Regional setting and location of study area covering the CALE sectors E, F and G. Basemap with bathymetry and topography from Jakobsson et al. (2012).

Figure 2

Location of regional transects 1-6 (Figs. 6-11) within area covered by the 3D lithosphere scale model of Klitzke et al. (2015). Bathymetry/topography based on Jakobsson et al. (2012). Bj: Bjørnøya; GR: Gakkel Ridge; KR: Knipovich Ridge; MJR: Morris Jessup Rise; PS: Pechora Sea; YP: Yermak Plateau.

Figure 3

(a) Free-air gravity anomalies within the study area based on Pavlis et al. (2012). (b) Magnetic anomalies anomalies within the study area based on Gaina et al. (2011). Present plate boundary, continent-ocean boundaries and location of regional transects 1-6 (Figs. 6-11) also shown.

Figure 4

(a) Depth to basement and main structural elements based on Klitzke et al. (2015). (b) Basement provinces within the study area. Present plate boundary, continent-ocean boundaries and location of regional transects 1-6 (Figs. 6-11) also shown. BB: Bjørnøya Basin; EB: Eurasia Basin; EBB: East Barents Basin; FH: Fedynsky High; FP: Finnmark Platform; GR: Gakkel Ridge; KR: Knipovich Ridge; Loppa High; MJR: Morris Jesup Rise; NB: Nordkapp Basin; NGS: Norwegian-Greenland Sea; NKB: North Kara Basin; NSA: North Siberian Arch; OB: Olga Basin; PB: Pechora Basin; PK: Pai Khoi; SeH: Sentralbanken High; SH: Stappen High; SKB: South Kara Basin; StH: Storbanken High; TB: Tromsø Basin; VVP: Vestbakken Volcanic Province; YP: Yermak Plateau.

Figure 5

(a) Depth to Moho based on Klitzke et al. (2015). (b) Depth to the lithosphere-asthenosphere boundary (LAB) based on Klitzke et al. (2015). Present plate boundary, continent-ocean boundaries and location of regional transects 1-6 (Figs. 6-11) also shown.

Figure 6

Regional Transect 1 from the Norwegian-Greenland Sea to Pai Khoi at both crustal and lithospheric scales. Transect location shown in Figs. 2-5. Based on 3D model of Klitzke et al. (2015) and additional references given in Table 1. BB: Bjørnøya Basin; KR: Knipovich Ridge; Loppa High; NB: Nordkapp Basin; PK: Pai Khoi: VVP: Vestbakken Volcanic Province. Salt diapirs within the Nordkapp Basin shown in black. See Table 1 for references.

Figure 7

Regional Transect 2 from the Norwegian-Greenland Sea to the Kara Sea at both crustal and lithospheric scales. Transect location shown in Figs. 2-5. Based on 3D model of Klitzke et al. (2015) and additional references given in Table 1. KR: Knipovich Ridge.

Figure 8

Regional Transect 3 from the Norwegian-Greenland Sea to Taimyr at both crustal and lithospheric scales. Transect location shown in Figs. 2-5. Based on 3D model of Klitzke et al. (2015) and additional references given in Table 1. KR: Knipovich Ridge.

Figure 9

Regional Transect 4 from Mezen Bay/Kanin Peninsula to Severnaya Zemlya at both crustal and lithospheric scales. Transect location shown in Figs. 2-5. Based on 3D model of Klitzke et al. (2015) and additional references given in Table 1. NSA: North Siberian Arch.

Figure 10

Regional Transect 5 from Baltic Shield/Fennoscandia to Eurasia Basin at both crustal and lithospheric scales. Transect location shown in Figs. 2-5. Based on 3D model of Klitzke et al. (2015) and additional references given in Table 1. FH: Fedynsky High; FP: Finnmark Platform; GR: Gakkel Ridge; NB: Nansen Basin; OB: Olga Basin; SeH: Sentralbanken High; StH: Storbanken High; TKF: Trollfjord-Komagelva Fault.

Figure 11

Regional Transect 6 from Northern Norway (Troms) to Morris Jessup Rise at both crustal and lithospheric scales. Transect location shown in Figs. 2-5. Based on 3D model of Klitzke et al. (2015) and additional references given in Table 1. AB: Amundsen Basin; BB: Bjørnøya Basin; Bj: Bjørnøya; GR: Gakkel Ridge; MJR: Morris Jesup Rise; NB: Nansen Basin; SH: Stappen High; TB: Tromsø Basin; VH: Veslemøy High; YP: Yermak Plateau. Salt diapirs within the Tromsø Basin shown in black.

Tables

Table 1

Principal references and data sources for construction of the regional transects 1-6 (Figs. 6-11).

Table 2

Tectonic synthesis of the greater Barents-Kara Sea region.

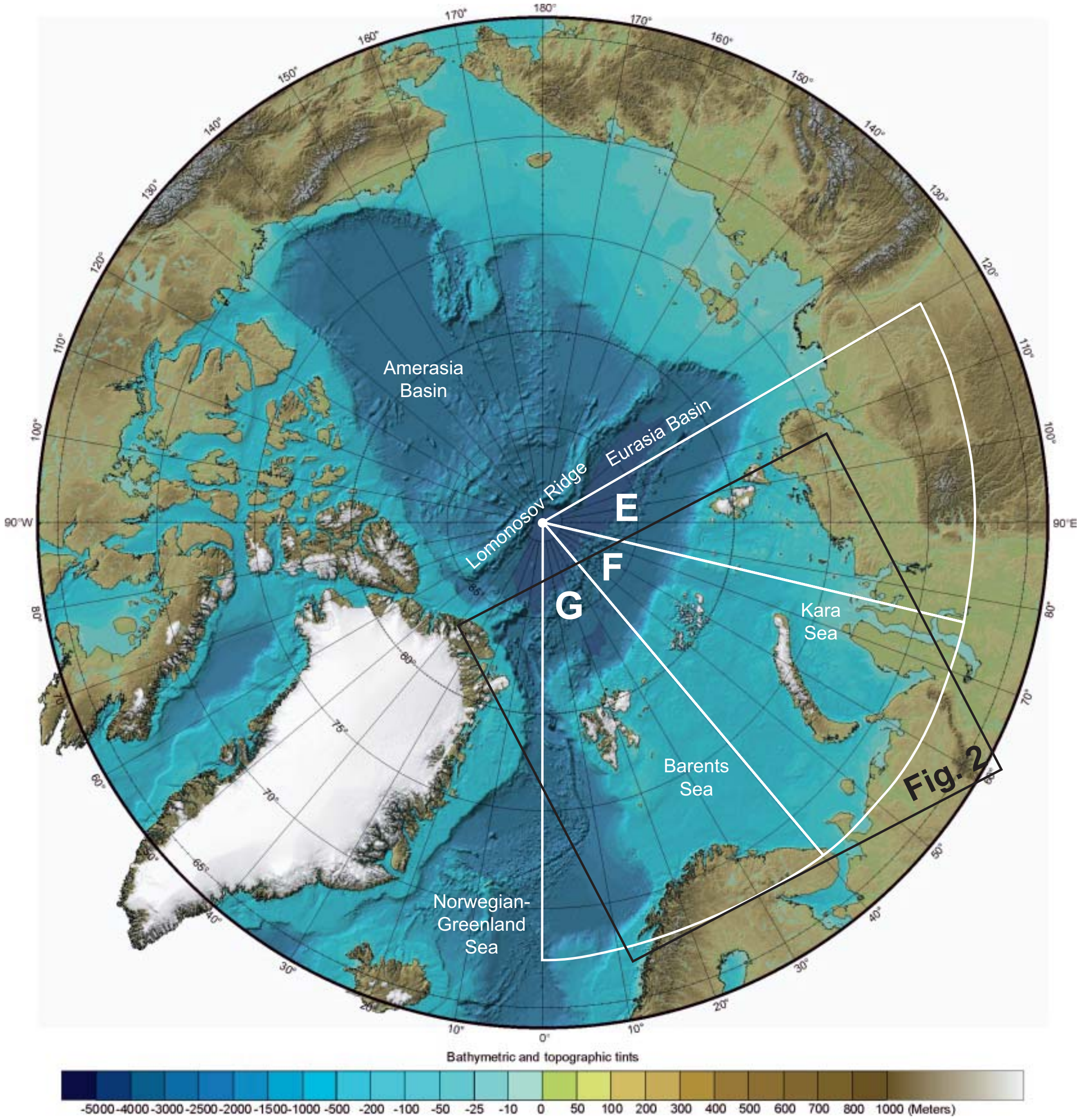

Amerasia Basin
Eurasia Basin
Lomonosov Ridge
E
F
G
Kara Sea
Barents Sea
Norwegian-Greenland Sea
Fig. 2
90°W
90°E
180°
0°
Bathymetric and topographic tints
-5000 -4000 -3000 -2500 -2000 -1500 -1000 -500 -200 -100 -50 -25 -10 0 50 100 200 300 400 500 600 700 800 1000 (Meters)

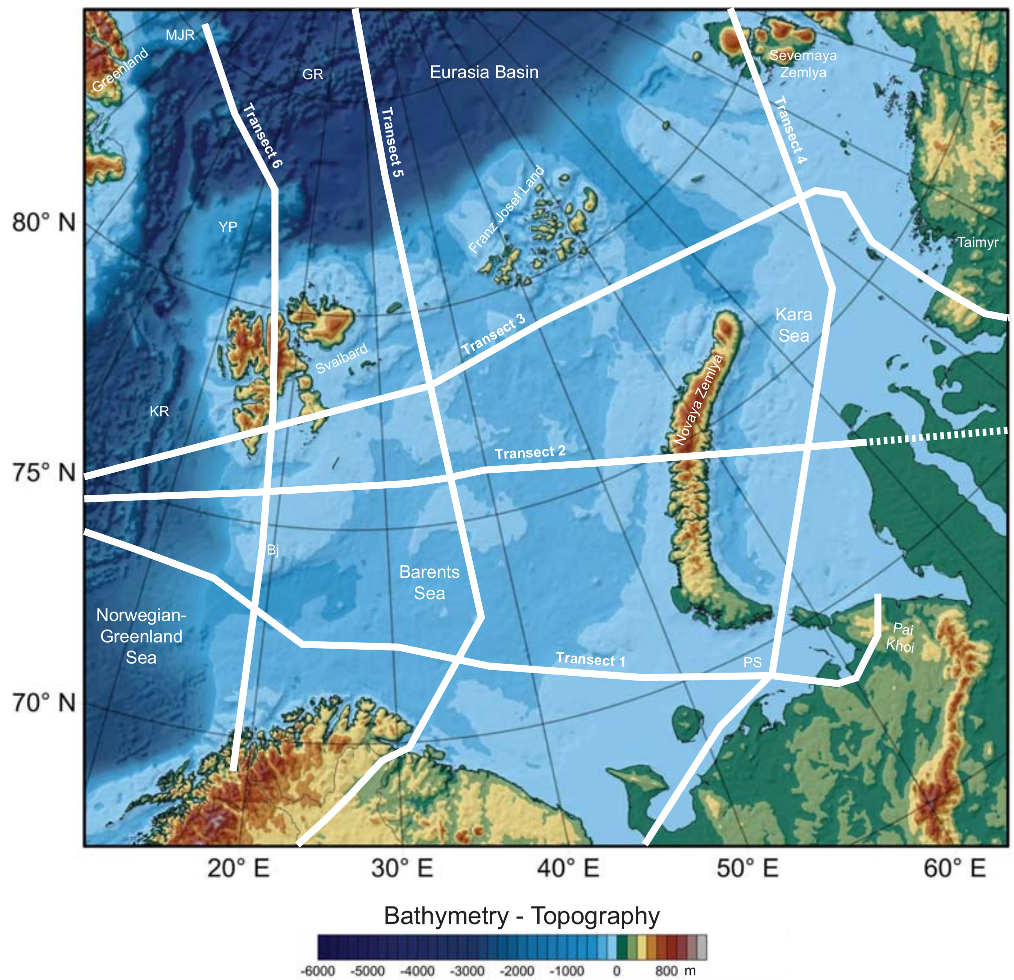

Greenland
MJR
GR
Eurasia Basin
Severnaya
Zemlya
Transect 6
Transect 5
Transect 4
Franz Josef Land
YP
Taimyr
Kara
Sea
Transect 3
Svalbard
Novaya Zemlya
KR
Transect 2
Bj
Barents
Sea
Norwegian-
Greenland
Sea
Transect 1
PS
Pai
Khoi
80° N
75° N
70° N
20° E
30° E
40° E
50° E
60° E
Bathymetry - Topography
-6000
-5000
-4000
-3000
-2000
-1000
0
800 m

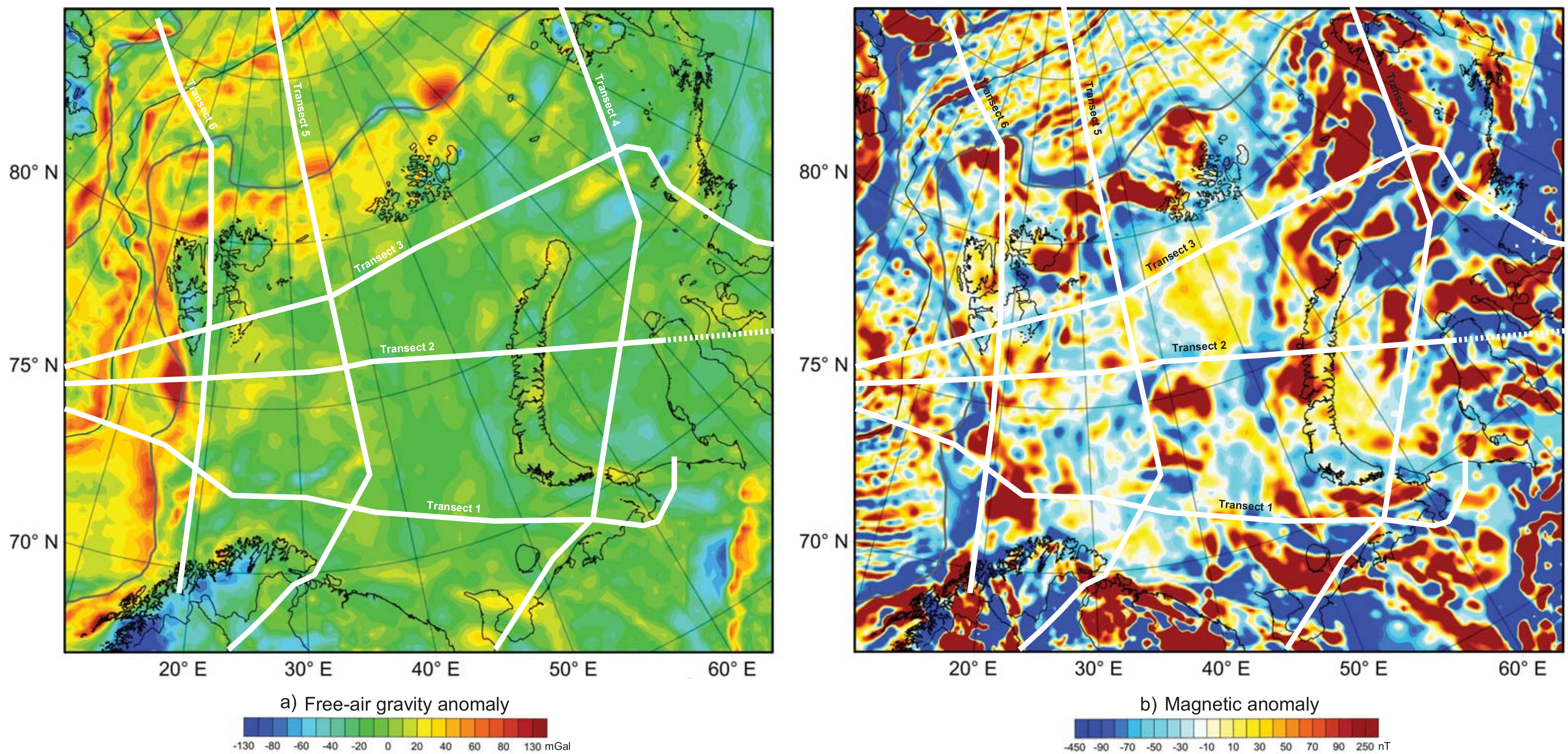

80° N
75° N
70° N
20° E
30° E
40° E
50° E
60° E
Transect 1
Transect 2
Transect 3
Transect 4
Transect 5
Transect 6
a) Free-air gravity anomaly
-130 -80 -60 -40 -20 0 20 40 60 80 130 mGal
b) Magnetic anomaly
-450 -90 -70 -50 -30 -10 10 30 50 70 90 250 nT

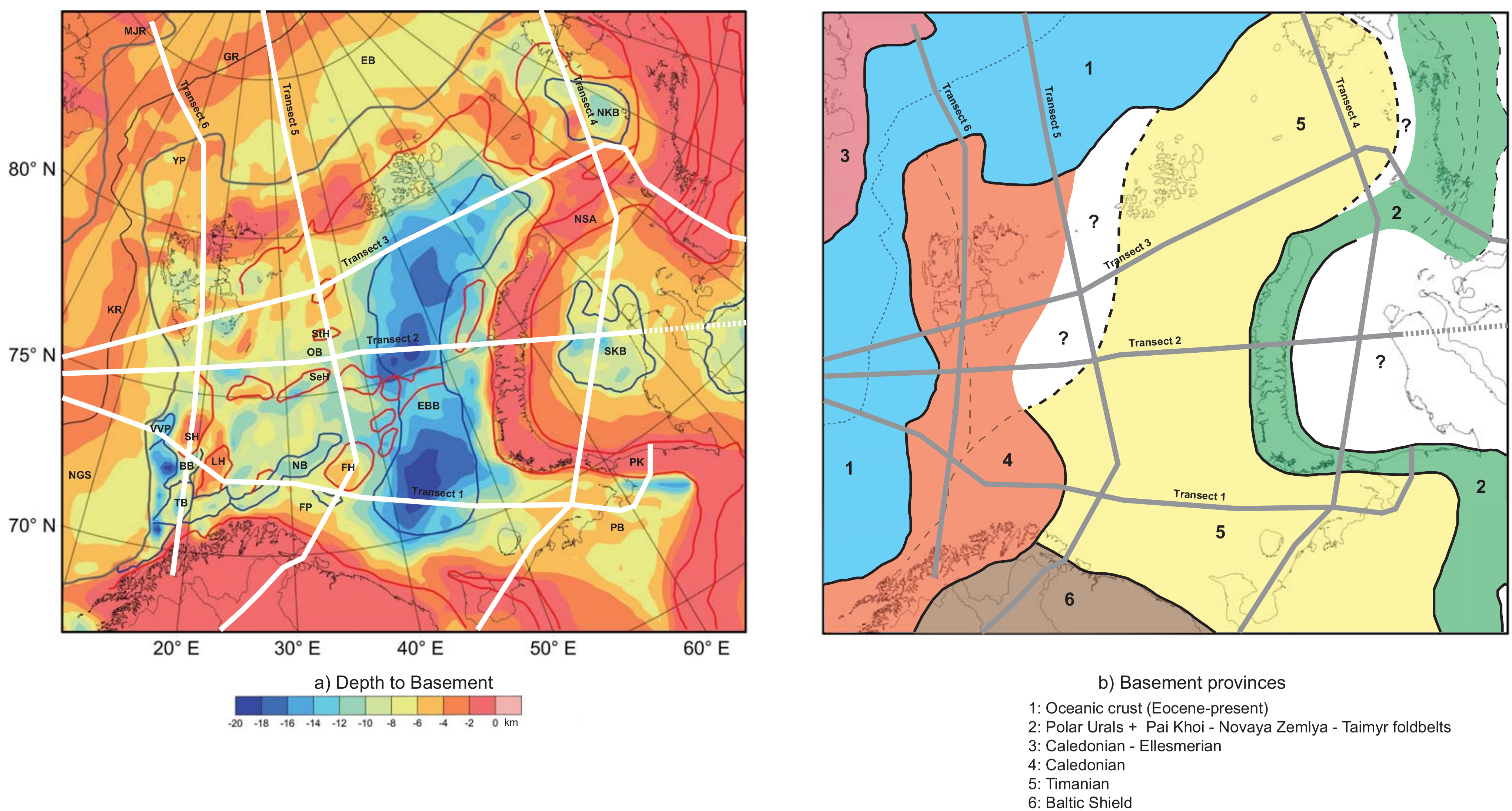
80° N
75° N
70° N
20° E
30° E
40° E
50° E
60° E
MJR
GR
EB
YP
KR
NGS
NKB
NSA
SKB
StH
OB
SeH
EBB
VVP
SH
BB
LH
TB
NB
FH
FP
PK
PB
Transect 1
Transect 2
Transect 3
Transect 4
Transect 5
Transect 6
a) Depth to Basement
-20 -18 -16 -14 -12 -10 -8 -6 -4 -2 0 km
1
2
3
4
5
6
?
b) Basement provinces
1: Oceanic crust (Eocene-present)
2: Polar Urals + Pai Khoi - Novaya Zemlya - Taimyr foldbelts
3: Caledonian - Ellesmerian
4: Caledonian
5: Timanian
6: Baltic Shield

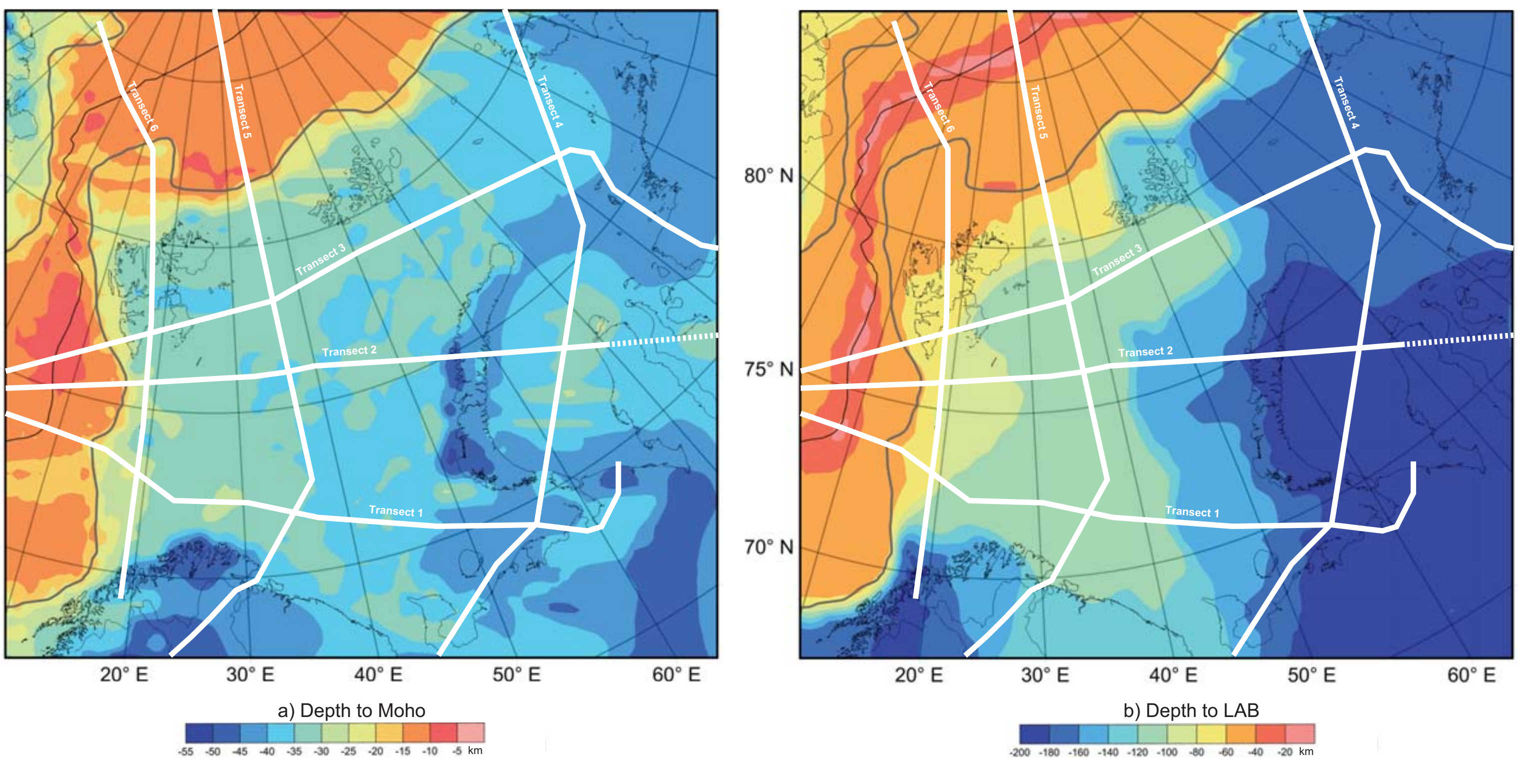

Transect 1
Transect 2
Transect 3
Transect 4
Transect 5
Transect 6
80° N
75° N
70° N
20° E
30° E
40° E
50° E
60° E
a) Depth to Moho
-55 -50 -45 -40 -35 -30 -25 -20 -15 -10 -5 km
b) Depth to LAB
-200 -180 -160 -140 -120 -100 -80 -60 -40 -20 km

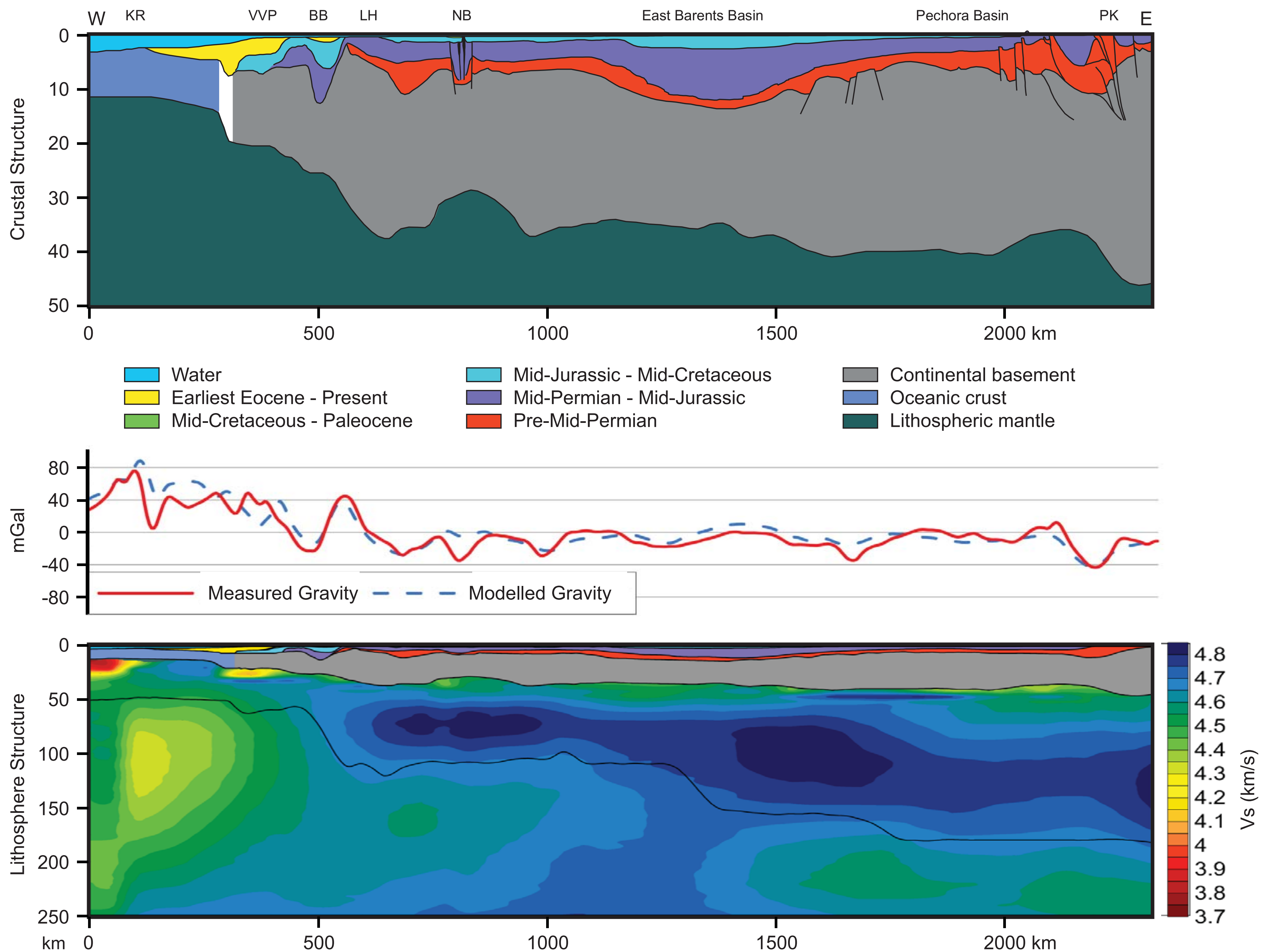
W
KR
VVP
BB
LH
NB
East Barents Basin
Pechora Basin
PK
E
Crustal Structure
0
10
20
30
40
50
0
500
1000
1500
2000 km
Water
Earliest Eocene - Present
Mid-Cretaceous - Paleocene
Mid-Jurassic - Mid-Cretaceous
Mid-Permian - Mid-Jurassic
Pre-Mid-Permian
Continental basement
Oceanic crust
Lithospheric mantle
mGal
80
40
0
-40
-80
Measured Gravity
Modelled Gravity
Lithosphere Structure
0
50
100
150
200
250
km
0
500
1000
1500
2000 km
4.8
4.7
4.6
4.5
4.4
4.3
4.2
4.1
4
3.9
3.8
3.7
Vs (km/s)

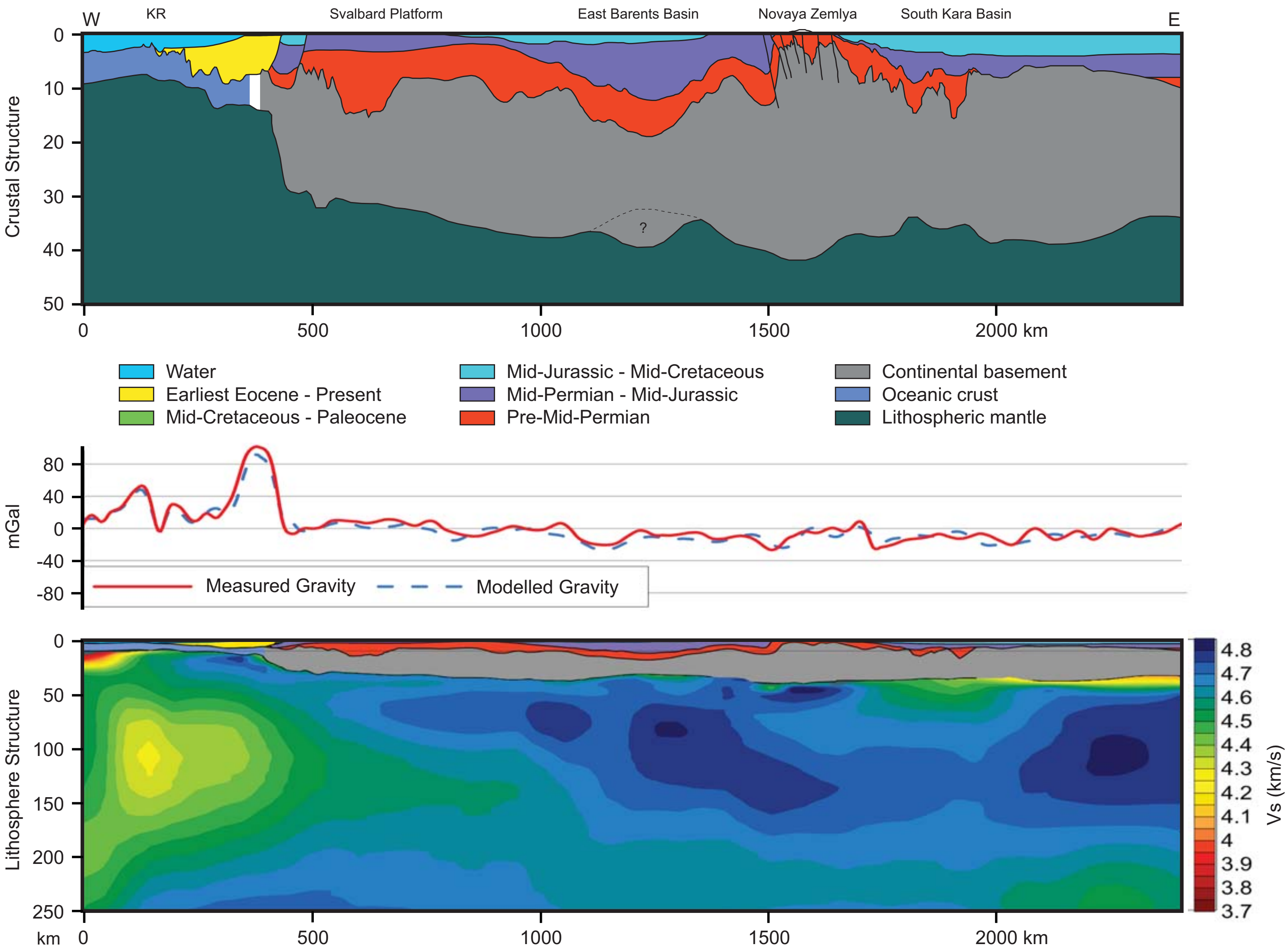
W
KR
Svalbard Platform
East Barents Basin
Novaya Zemlya
South Kara Basin
E
Crustal Structure
0
10
20
30
40
50
?
0
500
1000
1500
2000 km
Water
Earliest Eocene - Present
Mid-Cretaceous - Paleocene
Mid-Jurassic - Mid-Cretaceous
Mid-Permian - Mid-Jurassic
Pre-Mid-Permian
Continental basement
Oceanic crust
Lithospheric mantle
mGal
80
40
0
-40
-80
Measured Gravity
Modelled Gravity
Lithosphere Structure
0
50
100
150
200
250
km
0
500
1000
1500
2000 km
Vs (km/s)
4.8
4.7
4.6
4.5
4.4
4.3
4.2
4.1
4
3.9
3.8
3.7

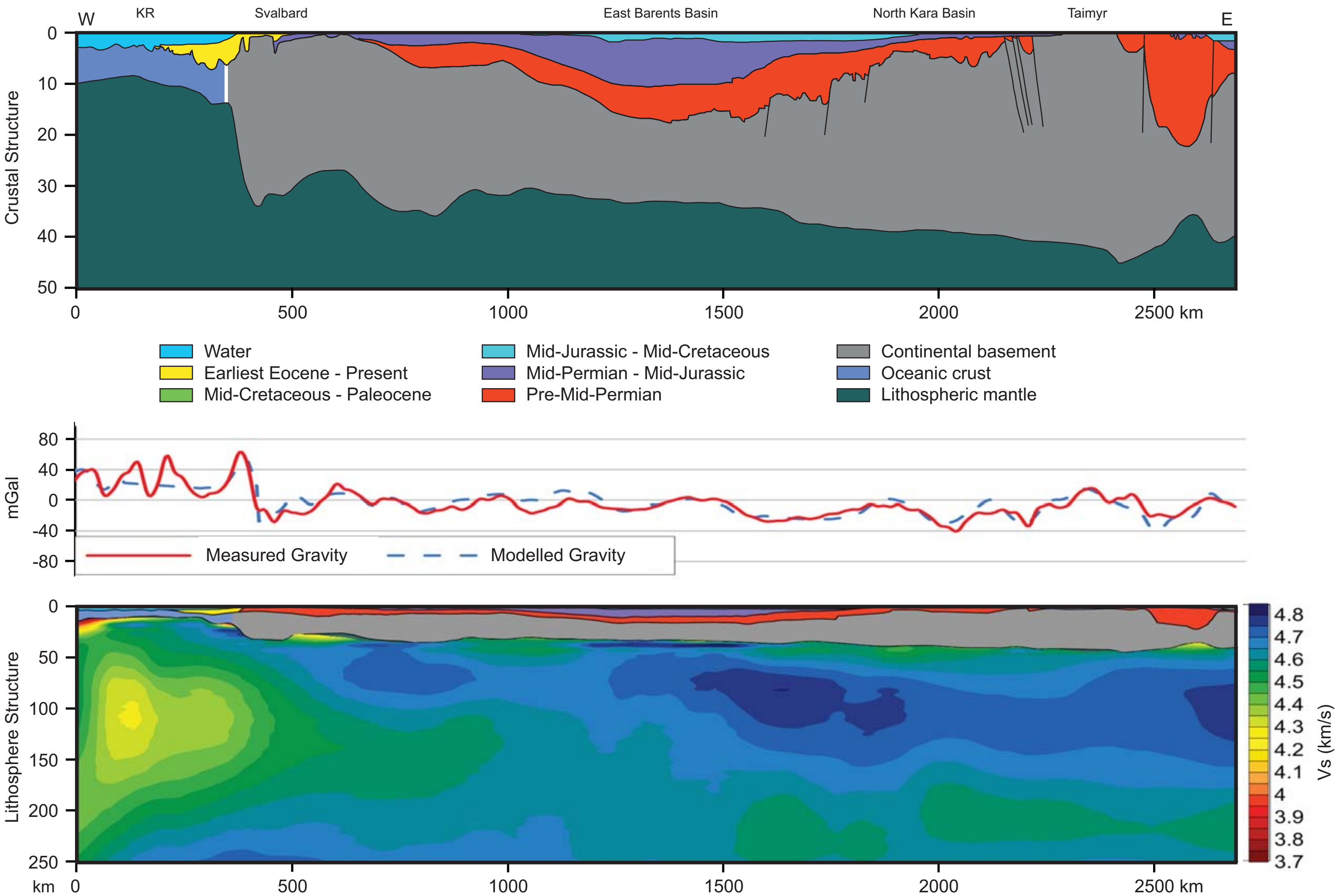

W
KR
Svalbard
East Barents Basin
North Kara Basin
Taimyr
E
Crustal Structure
0
10
20
30
40
50
0
500
1000
1500
2000
2500 km
Water
Earliest Eocene - Present
Mid-Cretaceous - Paleocene
Mid-Jurassic - Mid-Cretaceous
Mid-Permian - Mid-Jurassic
Pre-Mid-Permian
Continental basement
Oceanic crust
Lithospheric mantle
mGal
80
40
0
-40
-80
Measured Gravity
Modelled Gravity
Lithosphere Structure
0
50
100
150
200
250
km
Vs (km/s)
4.8
4.7
4.6
4.5
4.4
4.3
4.2
4.1
4
3.9
3.8
3.7

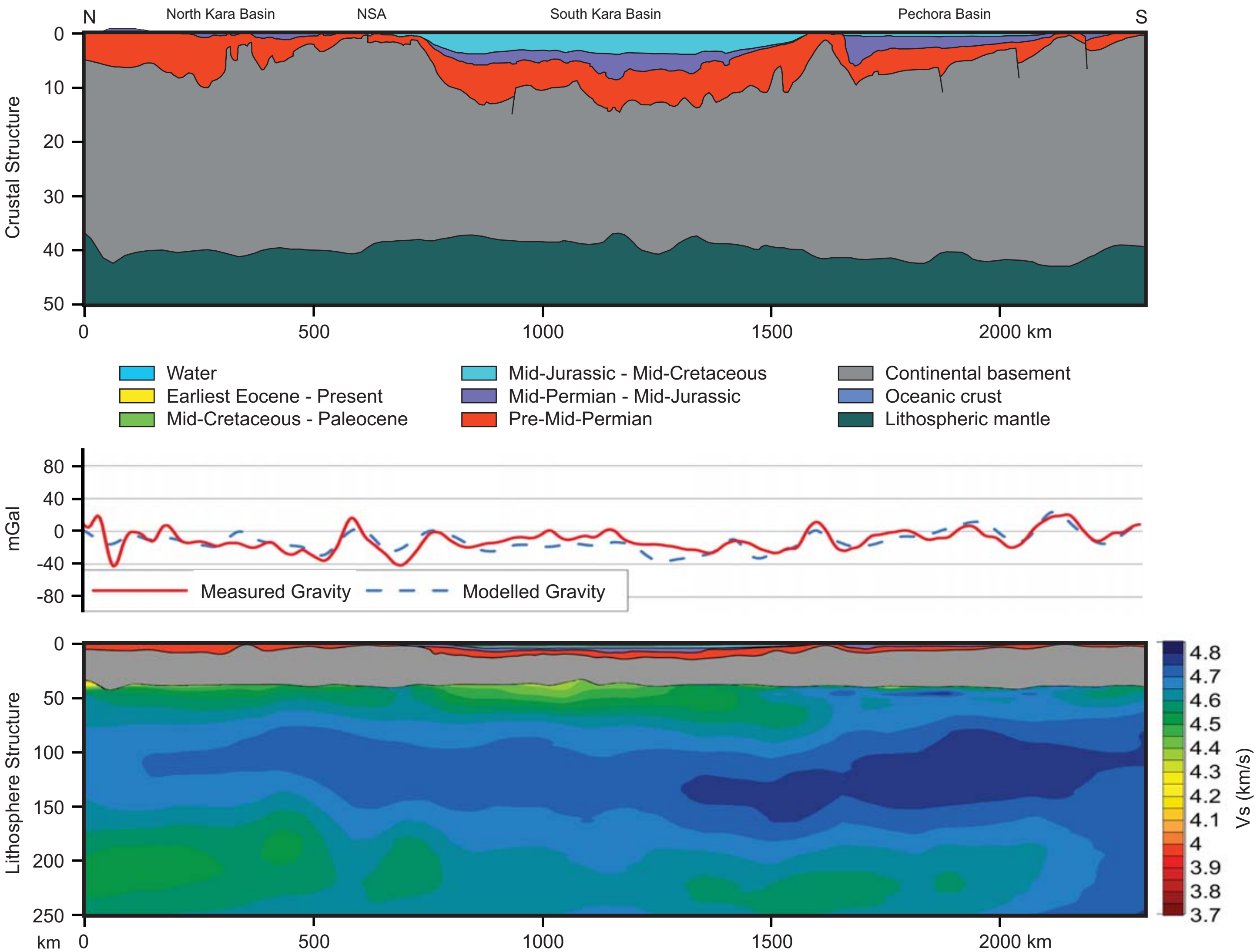
N
North Kara Basin
NSA
South Kara Basin
Pechora Basin
S
Crustal Structure
0
10
20
30
40
50
0
500
1000
1500
2000 km
Water
Earliest Eocene - Present
Mid-Cretaceous - Paleocene
Mid-Jurassic - Mid-Cretaceous
Mid-Permian - Mid-Jurassic
Pre-Mid-Permian
Continental basement
Oceanic crust
Lithospheric mantle
mGal
80
40
0
-40
-80
Measured Gravity
Modelled Gravity
Lithosphere Structure
0
50
100
150
200
250
km
Vs (km/s)
4.8
4.7
4.6
4.5
4.4
4.3
4.2
4.1
4
3.9
3.8
3.7

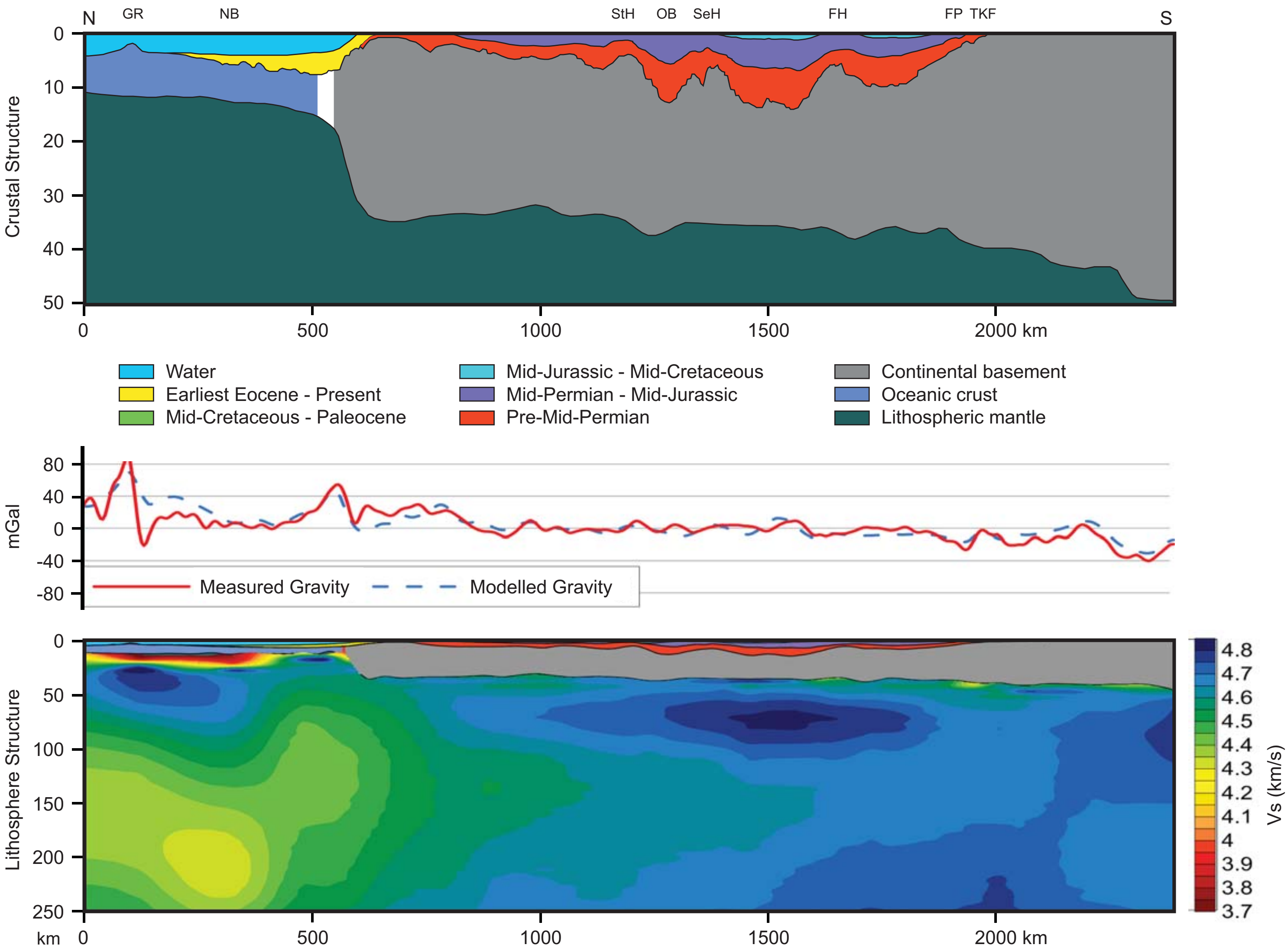
N
GR
NB
StH
OB
SeH
FH
FP
TKF
S
Crustal Structure
0
10
20
30
40
50
0
500
1000
1500
2000 km
Water
Earliest Eocene - Present
Mid-Cretaceous - Paleocene
Mid-Jurassic - Mid-Cretaceous
Mid-Permian - Mid-Jurassic
Pre-Mid-Permian
Continental basement
Oceanic crust
Lithospheric mantle
mGal
80
40
0
-40
-80
Measured Gravity
Modelled Gravity
Lithosphere Structure
0
50
100
150
200
250
km
0
500
1000
1500
2000 km
Vs (km/s)
4.8
4.7
4.6
4.5
4.4
4.3
4.2
4.1
4
3.9
3.8
3.7

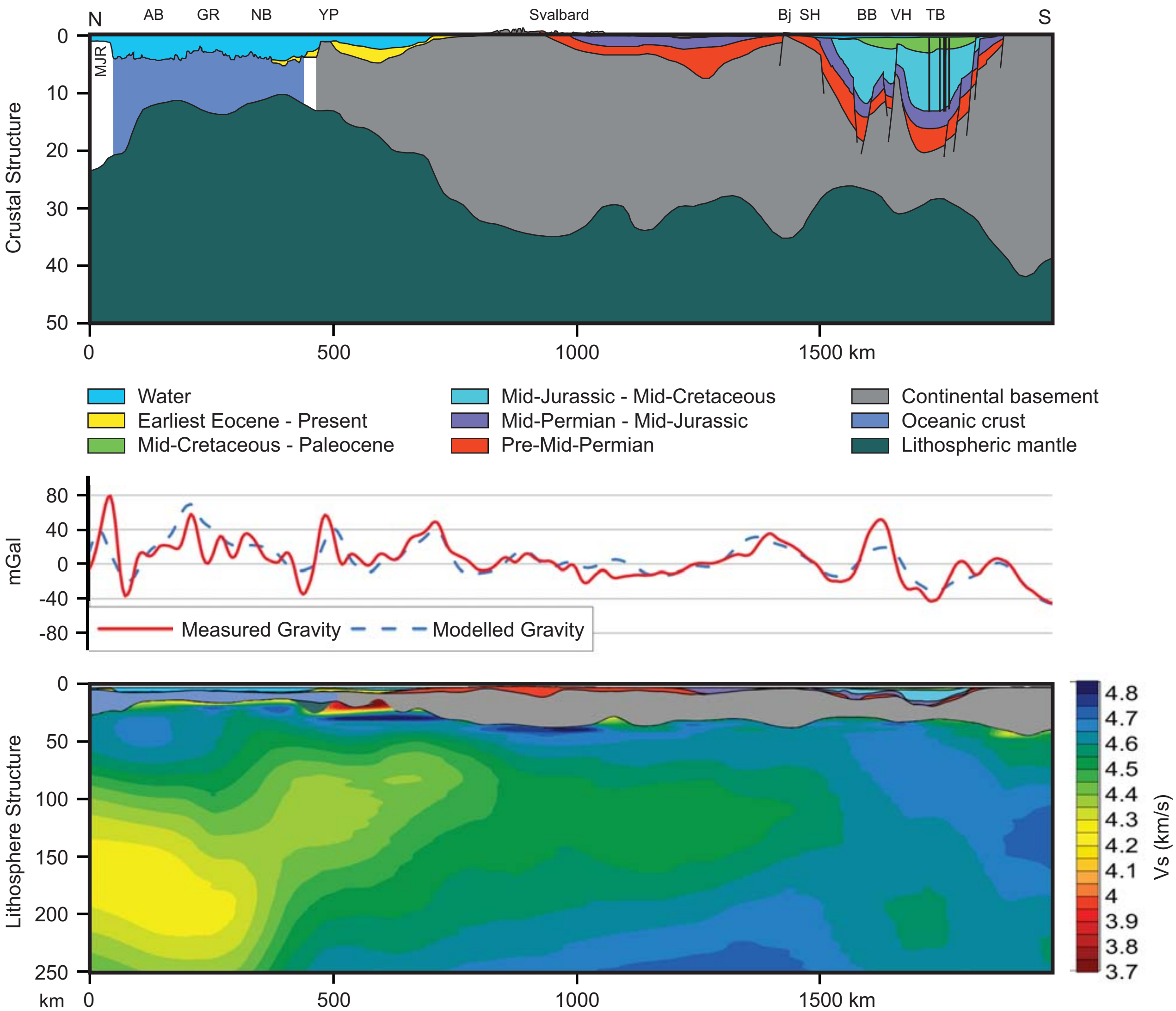
N
AB
GR
NB
YP
Svalbard
Bj
SH
BB
VH
TB
S
MJR
Crustal Structure
0
10
20
30
40
50
0
500
1000
1500 km
Water
Earliest Eocene - Present
Mid-Cretaceous - Paleocene
Mid-Jurassic - Mid-Cretaceous
Mid-Permian - Mid-Jurassic
Pre-Mid-Permian
Continental basement
Oceanic crust
Lithospheric mantle
mGal
80
40
0
-40
-80
Measured Gravity
Modelled Gravity
Lithosphere Structure
0
50
100
150
200
250
km
Vs (km/s)
4.8
4.7
4.6
4.5
4.4
4.3
4.2
4.1
4
3.9
3.8
3.7

Table 1 Principal references and data sources

Transect	Area	Key references
Transect 1	Norwegian-Greenland Sea - SW Barents Sea	Clark et al. (2013, 2014)
	Central and Eastern Barents Sea	Johansen et al. (1993)
	Pechora Basin – Pai Khoi	Sobornov (2013, 2015)
Transect 2	Norwegian-Greenland Sea – W Barents Sea	Breivik et al. (2003, 2005)
	E Barents Sea – Novaya Zemlya – S Kara Sea	Ivanova et al. (2011)
Transect 3	Norwegian-Greenland Sea	Ljones et al. (2004)
	Svalbard	Czuba et al. (2008)
	NW Barents Sea	Minakov et al. (2012b)
	N Barents Sea	Minakov et al. (*this volume*)
	NE Barents Sea – N Kara Sea	Ivanova et al. (2011)
	Taimyr	Afanasenkov et al. (2016)
Transect 4	Mezen Bay/Kanin Peninsula – Severnya Zemlya	Ivanova et al. (2011)
Transect 5	Onshore Fennoscandia	Lousto et al. (1989)
	S Barents Sea	Ivanova et al. (2011)
	Central Barents Sea	Khutorskoi et al. (2008)
	N Barents Sea – Eurasia Basin	Minakov et al. (2012a)
Transect 6	Northern Norway (Troms)	Indrevær et al. (2013)
	W Barents Sea – Svalbard	Jackson et al. (1993)
	Svalbard – Yermak Plateau – Morris Jessup Rise	Jokat et al. (1995)
		Geissler et al. (2011)

Table 2. Tectonic synthesis of the greater Barents-Kara Sea region.

TIME	**LOCATIONS** (west to east)											**TECTONIC EVENT**
(Ma)	*Sv*	*No*	*WBS*	*EBS*	*TP*	*FJL*	*SNZ*	*NNZ*	*NKS*	*SKS*	*T*	
0	*v v v*											Miocene to present extension
20												
40												Paleogene transpression and compression (Spitsbergen-Eurekan FTB)
60	*v v v*											
80												Late Cretaceous-Paleocene extension
100												
120	*v v v*		*v v v*	*v v v*		*v v v*						High Arctic LIP
140												Late Jurassic-Early Cretaceous extension
160												
180												
200				***???***						***???***		Late Triassic (-?Early Jurassic) compression (Taimyr and Novaya Zemlya FTB)
220												
240												
260										*v v v*	***???***	Permo-Triassic extension
280				***???***						***???***		Late Carboniferous- Permian compression (Uralian orogenesis)
300												
320												Late Carboniferous extension
340												L Devonian-E Carboniferous compression (Ellesmerian-Svalbardian collision)
360												
380		*v v v*		*v v v*	*v v v*							Devonian extension (460-420) (post-orogenic collapse and/or rifting)
400												
420				***???***								Silurian-Devonian compression (Caledonian orogenesis)
440												
460												
480												Cambro-Ordovician extension (basin subsidence)
500												
520												Neoproterozoic to late Cambrian compression (Timanian orogenesis)
540												

Notes: FJL: Franz Josef Land; FTB: Fold and thrust belt; No: Norway; NNZ: Northern Novaya Zemlya; NKS: North Kara Sea; SKS: South Kara Sea; T: Taimyr; TP: Timan-Pechora; EBS: East Barents Sea; WBS: West Barents Sea; SNZ: Southern Novaya Zemlya; Sv: Svalbard; v v v = magmatism; dark grey = compressional deformation and lighter grey = extensional deformation; *???* = speculative.